CellPress OPEN ACCESS

Trends in Biotechnology

Research Article

Engineering environmental bacteria for whole-cell PET hydrolysis and assimilation

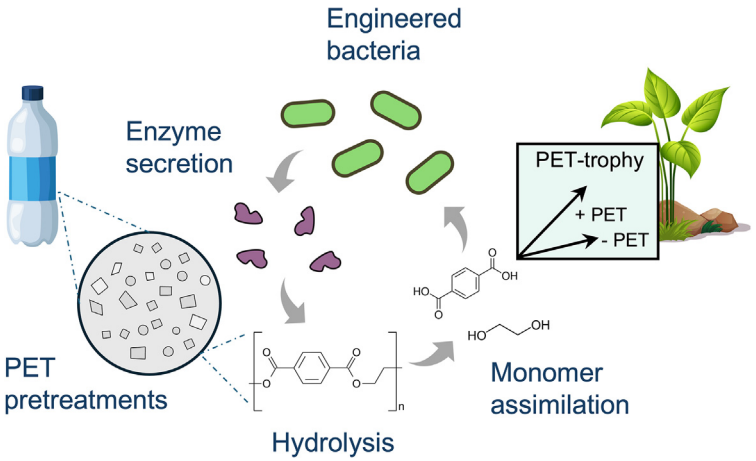

We report the engineering of environmental bacteria for the direct consumption of poly(ethylene terephthalate) plastic through the production of enzymes for plastic breakdown and the exploitation of their natural ability to assimilate the resulting degradation products. This self-sustained consumption of plastic enables the breakdown of microplastics in urban wastewater.

Alice M. Banks, Umar Abdulmutalib, Brooke Wain, Christian Sonnendecker, Harry Doherty, Zheren Zhang, Juhyun Kim, Charlotte Bosomworth, Stuart Brown, Ren Wei, Carolina Álvarez-Ortega, Pablo Pomposiello, Claudio Avignone-Rossa, Gerald Larrouy-Maumus, Wolfgang Zimmermann, José I. Jiménez

j.jimenez@imperial.ac.uk (J.I. Jiménez).

Highlights

We have systematically investigated bottlenecks in the development of whole-cell catalysts for the biodegradation of poly(ethylene terephthalate) plastic.

Poly(ethylene terephthalate)-hydrolysing enzymatic activity, secretion, and plastic bioavailability limit microbial growth.

An environmental bacterial strain of *Pseudomonas umsongensis,* capable of assimilating terephthalic acid, was engineered to secrete the poly(ethylene terephthalate) hydrolase polyester hydrolase Leipzig 7.

The engineered strain can use poly (ethylene terephthalate) as the main nutrient, requiring long incubations and a solvent-treated substrate.

The engineered strain can break down poly(ethylene terephthalate) microplastics when added to wastewater.

Trends in Biotechnology, Month 2026, Vol. xx, No. xx
https://doi.org/10.1016/j.tibtech.2026.06.008

Trends in Biotechnology

CellPress OPEN ACCESS

Research Article

Engineering environmental bacteria for whole-cell PET hydrolysis and assimilation

Alice M. Banks [1,#], Umar Abdulmutalib [2,3,#], Brooke Wain [1,4,#], Christian Sonnendecker [5], Harry Doherty [1], Zheren Zhang [1,6], Juhyun Kim [7], Charlotte Bosomworth [1], Stuart Brown [2], Ren Wei [8,11], Carolina Álvarez-Ortega [9], Pablo Pomposiello [9], Claudio Avignone-Rossa [2], Gerald Larrouy-Maumus [10], Wolfgang Zimmermann [5], and José I. Jiménez [1,4,*]

Poly(ethylene terephthalate) (PET) is one of the most widely used plastics in food and textile applications, yet post-consumer PET waste persists and accumulates in the environment as macro- and microplastics with adverse health and ecological impacts. Although PET-hydrolysing enzymes have been extensively studied *in vitro*, whole-cell microbial systems capable of using PET as a growth substrate remain limited, particularly for difficult-to-collect waste. Here, we engineer an environmental bacterium to directly assimilate PET. A strain of *Pseudomonas umsongensis* capable of metabolising the PET monomer terephthalic acid was isolated and engineered to secrete the high-activity PET hydrolase polyester hydrolase Leipzig 7 via a recombinant twin-arginine translocation motif signal peptide. PET bioavailability was further enhanced through solvent-based pretreatment to generate an amorphous, macroporous substrate. The engineered strain demonstrated direct PET utilisation and hydrolysis, supporting self-sustaining microbial growth. Additionally, in non-sterile wastewater the strain survived and hydrolysed PET microplastics, highlighting its potential for bioremediation and sustainable upcycling applications.

Introduction

Commonly used plastics are nonbiodegradable materials that accumulate in the environment and pose a health hazard across almost every ecosystem on the planet [1]. The plastic poly(ethylene terephthalate) (PET), in particular, is a versatile material used in multiple applications, ranging from food and beverage packaging to textile production [2]. Compared to other plastics, PET has relatively high collection rates and can be recycled by mechanical and chemical methods [3]. However, due to its widespread use and the difficulty of collecting certain PET waste streams, such as fibres released from fabrics, PET frequently leaks into the environment [4,5] where it poses significant health and ecological risks [6].

Biological recycling of PET that has reached its end of life and cannot be recycled mechanically has been proposed as a mitigation strategy to reduce environmental pollution while conserving fossil resources [7]. This approach relies on enzymes that catalyse the breakdown of polyester plastics under mild reaction conditions compared to conventional chemical processes. Among commonly used plastics, PET is currently the only one being processed at a pilot industrial scale using enzymatic recycling technologies [8]. These processes involve the *in vitro* enzymatic hydrolysis of PET, yielding large quantities of the PET constituent monomers terephthalic acid (TA) and ethylene glycol (EG) [9–11]. While these monomers can be repolymerised to generate virgin PET, they can also serve as carbon and energy sources for microbial growth [12] or be

Technology readiness

There is a significant amount of work reporting the use of enzymes for *in vitro* poly(ethylene terephthalate) hydrolysis. Albeit in lower numbers, whole-cell methods for 'one-pot' plastic hydrolysis have also been developed. They all have in common the need for an additional carbon source in order to obtain high biomass so that enough poly(ethylene terephthalate)-degrading enzymes accumulate in the culture broth and hydrolysis can take place. The idea of linking hydrolysis to microbial metabolism is, in our opinion, more interesting, as it not only allows the direct upcycling of plastic waste but also enables the efficient biodegradation of plastics that are difficult to collect, such as microplastics.

Our findings suggest that rationally engineered bacteria that can metabolise poly(ethylene terephthalate) monomers can be used for the direct use of plastic as the main carbon source under lab conditions, achieving a technology readiness level of 4. Moreover, we also demonstrate the potential of this technology for the removal of microplastics added to wastewater samples in the lab (technology readiness level of 4), paving the way for the deployment of the technology in more relevant environments.

[1]Department of Life Sciences, Imperial College London, South Kensington, London SW7 2AZ, UK
[2]Discipline of Microbes, Infection and Immunity, School of Biosciences, Faculty of Health and Medical Sciences, University of Surrey, Guildford GU2 7XH, UK

converted into value-added products in a process known as **upcycling** (see Glossary) [13–18]. This two-step approach, comprising *in vitro* enzymatic hydrolysis followed by *in vivo* microbial conversion (see [19,20]), requires the initial expression and purification of appropriate enzymes in large amounts to reach a standard enzyme loading of 0.5–3 mg of enzyme per gram of PET [21], increasing both the energy and carbon footprint of the process and reducing the potential economic viability of biological PET waste valorisation [22].

In this research article, we describe the *in vivo*, or direct, hydrolysis of PET (Figure 1A). This process has been proposed to improve both the sustainability and economic viability of PET recycling, as well as serve as a potential solution to reduce microplastic pollution in waterways and agricultural land when applied in wastewater (WW) treatment contexts [23–25]. Previous studies have reported the engineering of different microbial hosts for the recombinant expression and secretion of PET hydrolases capable of breaking down PET when cultured in the presence of alternative growth substrates, as reviewed recently by Liu *et al.* [26], as well as their use to break down PET in soils [27]. None of these systems, however, can sustain growth when PET is the main nutrient.

The ability to grow primarily on PET as a carbon source, with minimal supplementation by additional nutrients—a process also referred to as '**PET-trophy**' [28]—is exemplified by the bacterium *Ideonella sakaiensis* (recently reclassified as *Piscinibacter sakaiensis*; hereafter referred to as *I. sakaiensis* to maintain consistency with established protein nomenclature, e.g., IsPETase), which was isolated from a plastic recycling plant [11]. *I. sakaiensis* is not, however, an organism that is easy to culture or manipulate in the laboratory due, among other factors, to its limited secretion capabilities [29]. As a result, previous work has advocated for the modification of established biotechnological workhorses, such as *Pseudomonas putida*, for PET hydrolysis, assimilation of the monomers TA and EG [28,30], and upcycling into value-added products such as muconate [31]. However, the goal of engineering a bacterium that can use PET as its main growth substrate has not been achieved to date.

This bottom-up approach is useful for identifying limiting steps in the process, which can then be optimised using existing molecular tools available for genetically tractable microbial hosts. In this work, we succeeded in engineering an environmental isolate for PET assimilation by following three key steps: screening and isolation of bacteria able to use TA as a sole carbon source; generation of broad-host plasmids enabling the expression and efficient secretion of PET hydrolases; and pretreatment of PET to increase substrate bioavailability. Our results show that systematic investigation of these key processes can lead to overall optimisation of PET biodegradation, resulting in strains capable of using PET as a growth substrate, and represent a first step towards *in vivo* PET hydrolysis at scale. Moreover, our engineered strains were able to hydrolyse PET microplastics in WW, highlighting their potential for **bioremediation** applications.

Results

Isolation and growth characterisation of candidate microbial strains

Microbial strains were isolated from environmental samples taken from grassland, soil, and pond locations using TA for culture enrichment. As a result of the screening, we isolated six new bacterial strains able to grow on TA as the sole carbon source in pure cultures. These strains were sequenced completely and classified according to their 16S rRNA sequence as *Acinetobacter schindleri* LK1, *Rhodococcus* sp. HM1, *Pseudomonas umsongensis* GS, *Pseudomonas umsongensis* HM2, *Pseudomonas azerbaijanoccidens* SH, and *Ralstonia insidiosa* TS. In addition to TA, we also tested their ability to use EG as a growth substrate (Figure 1B and Figure S1A).

[3]Department of Biological Sciences, Faculty of Science, Northwest University, Kano, Muhammad Buhari Way, PM 3220 Kabuga, Kano State, Nigeria
[4]Imperial Centre for Engineering Biology, Imperial College London, South Kensington, London SW7 2AZ, UK
[5]Institute of Analytical Chemistry, Leipzig University, Leipzig 04103, Germany
[6]School of Biological and Behavioural Sciences, Queen Mary University of London, London E1 4NS, UK
[7]School of Life Sciences, BK21 FOUR KNU Creative BioResearch Group, Kyungpook National University, Daegu 41566, Republic of Korea
[8]Department of Microbiology and Bioprocess Technology, Institute of Biochemistry, Leipzig University, Johannisallee 21-23, Leipzig 04103, Germany
[9]Bacmine, Calle de Santiago Grisolía, Tres Cantos 28760, Spain
[10]Centre for Bacterial Resistance Biology, Department of Life Sciences, Faculty of Natural Sciences, Imperial College London, London SW7 2AZ, UK
[11]Institute of Applied Microbiology, RWTH Aachen University, Aachen, Germany
[#]Equal contribution

*Correspondence:
j.jimenez@imperial.ac.uk (J.I. Jiménez).

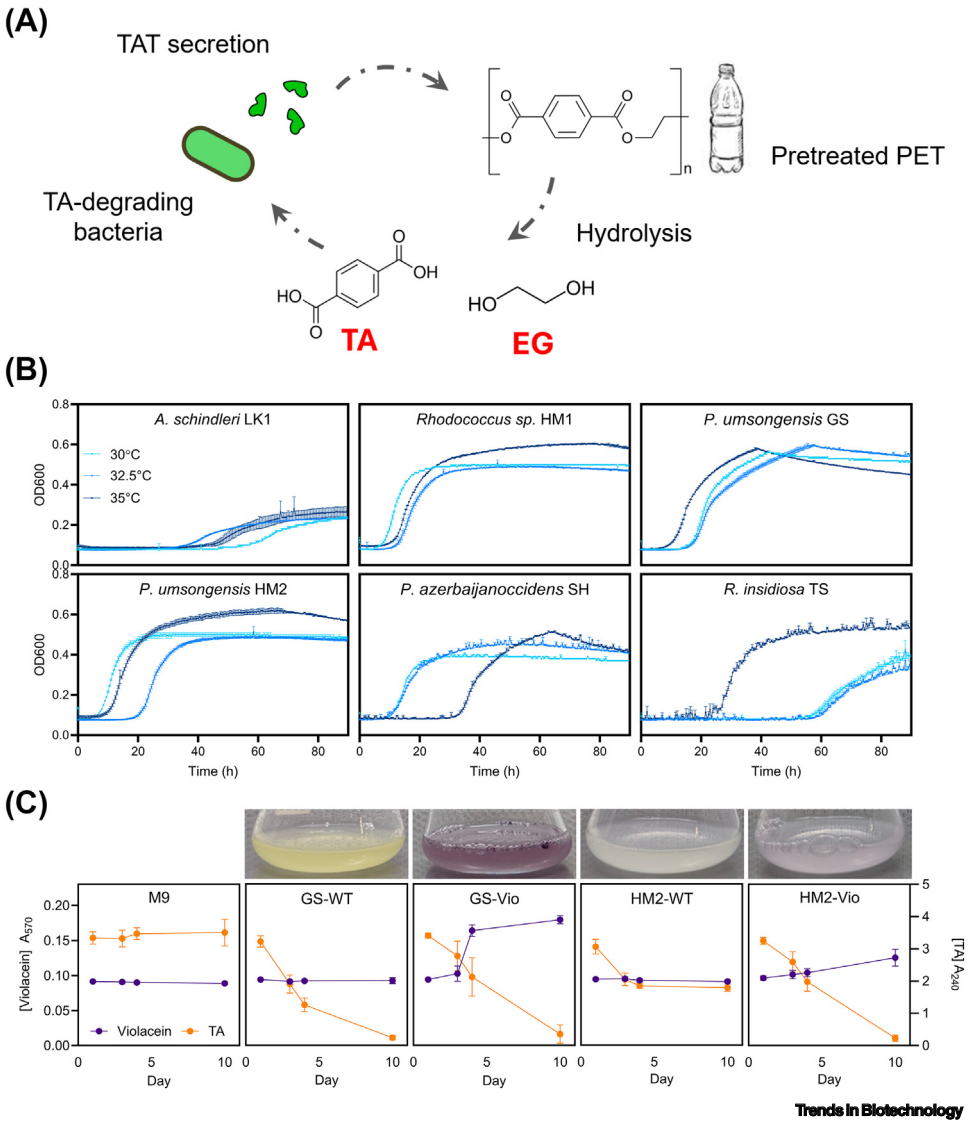

Figure 1. PET valorisation by environmental isolates. (A) diagram outlining the general strategy followed in this work. TA and EG stand for, respectively, terephthalic acid and ethylene glycol. (B) Growth of environmental isolates *A. schindleri LK1, Rhodococcus sp. HM1, P. umsongensis GS, P. umsongensis HM2, P. azerbaijanoccidens SH, and R. insidiosa TS*, using the PET monomer TA as the sole carbon source across a temperature range (also refer to Figure S1A,B). (C) The potential of the two *P. umsongensis* strains GS and HM2 for PET upcycling was assessed by transforming them with a plasmid containing the violacein biosynthetic pathway and monitoring the conversion of TA (yellow line) into violacein (purple line) over time (also refer to Figure S1C,D). Error bars denote the standard deviation (SD) of three biological replicates.

Isolates LK1, HM1, GS, HM2, SH, and TS all exhibited growth using TA as a sole carbon source; however, HM1 was the only isolate showing growth on EG. The *Pseudomonas* spp. (GS, HM2 and SH) and *Rhodococcus* sp. HM1 all reached a similar biomass using TA, with minor differences in growth rate under the conditions tested. *R. insidiosa* TS achieved a moderate biomass using TA as a sole carbon source and exhibited a longer lag phase than the *Pseudomonas* spp.

We conducted a genomic search of the genomes involved in TA metabolism in the environmental isolates. We investigated the presence of homologs for the *tphA1A2A3B* genes responsible for

Glossary

Bioremediation: the use of living organisms, typically microbial, for the removal of pollutants.
PET-trophy: the ability of microorganisms to hydrolyse PET plastic and assimilate the resulting monomers as nutrients.
Upcycling: the use of waste streams that would typically be discarded as feedstocks for other processes (biological in this case) so that they can be transformed into molecules with added value.
Whole-cell catalyst: a complete organism, typically microbial, that catalyses a chemical reaction. The required enzymes are produced by the organism as it grows, as opposed to being produced and purified elsewhere.

the conversion of TA into protocatechuate (PCA) [32] using the NCBI's BLASTp sequence comparison tool. This analysis revealed that isolates HM1, HM2, GS, and SH all contained gene clusters homologous to the *tph* operon (locus tags M1M07_11365 to 11370 for HM1, M1M10_17875 to 11885 for HM2, M1M08_06420 to 06430 for GS, and M1M11_02935 to 02945 for SH). The equivalent cluster was lacking in isolates LK1 and TS. At this stage, we discarded the Gram-positive HM1 and LK1, as no molecular tools for genetic manipulation were available for these strains. The remaining four environmental isolates were also screened for resistance to a panel of routinely used antibiotics (Figure S1B, in the Supplemental information online). *R. insidiosa* TS demonstrated resistance to all antibiotics tested apart from tetracycline, whereas isolate *A. schindleri* LK1 was found to be susceptible to the full range tested. *Pseudomonas* spp. (GS, HM2 and SH) only showed resistance to ampicillin, which is a common feature of the genus [33].

Based on initial growth characterisation and genome analysis, the isolates *P. umsongensis* GS and *P. umsongensis* HM2 were selected for further investigation due to their ability to grow on TA as a sole carbon source, their susceptibility to a wide range of antibiotics, and the possession of the *tph* gene cluster in the genome. Furthermore, these isolates are all *Pseudomonas* spp., a genus for which an extensive molecular toolkit is available.

We then tested the ability of the isolates *P. umsongensis* GS and HM2 to produce molecules of biotechnological interest using TA as a growth substrate. We used violacein as a proof of concept. Violacein has antitumoral and antimicrobial properties [34] and its biosynthetic pathway, composed of five genes, can be expressed recombinantly in diverse bacteria, including the EG degrader *P. putida* JM37 [35]. Violacein's purple colour makes it easy to track in production experiments. The plasmid pSEVA63-Hvio, carrying the violacein biosynthetic pathway [36], was delivered to both strains, which were cultured in M9 + TA and monitored over a 10-day period for the conversion of TA to violacein. The engineered strains demonstrated the conversion of TA to violacein. Wild-type (WT) cultures showed the depletion of TA over the 10-day incubation period but no accumulation of violacein. Strains carrying the pSEVA63-Hvio plasmid similarly demonstrated depletion of TA but also caused the accumulation of the violacein pigment (detectable at 570 nm), and the cultures developed a visible purple colour resulting from production (Figure 1C). Out of the two isolates tested, *P. umsongensis* GS showed the highest violacein production ability when expressing the recombinant pathway, suggesting it is a strong candidate host for PET hydrolase expression. Furthermore, when cultured using equimolar mixtures of TA EG in the mM range, the growth of GS was not affected, which supports its choice as a suitable organism for PET upcycling (Figure S1C). GS also exhibited faster growth and reached higher biomass growing on TA than a variant of *P. putida* KT2440 previously engineered for TA assimilation (Figure S1D) [30].

Engineering environmental isolates for the expression and secretion of PET hydrolases

There are a considerable number of enzymes active against PET reported in the literature [37]. We focused on two main groups for this work to assess whether they could support microbial growth on PET (Table S1, in the Supplemental information online). The first group comprises enzymes derived from PETase and MHETase of *I. sakaiensis*, a mesophilic proteobacterium, including variants engineered through directed evolution [38–40]. In contrast, the second group consists of enzymes sourced from thermophilic actinobacteria or identified through metagenomic screenings [9,10,41,42].

The enzymes studied in this work were originally used for cytoplasmic expression in *Escherichia coli* devoid of a signal peptide, which we introduced at the N terminus of each protein for their secretion in the environmental strains. Since all PET hydrolases tested have been successfully

expressed in the cytoplasm of *E. coli* [9,10,31–34], we therefore sought to take advantage of the type II secretion system of *Pseudomonas,* responsible for the extracellular secretion of folded proteins. To this end, we added the N-terminal signal peptide of the UxpB phosphatase of *P. putida* KT2440, encoded by PP_1043 [43] to each of the enzymes. In its native organism, the UxpB phosphatase is secreted extracellularly under low-phosphate conditions. UxpB is transported to the cell surface by the type II Xcp secretion system, via a 52-amino-acid signal peptide carrying a twin-arginine translocation (TAT) motif.

We tested the secretion of the enzymes in different Gram-negative species, including *E. coli* (used for cloning) and *P. putida* (the native organism of the signal peptide), as well as the environmental isolate *P. umsongensis* GS (Figure 2). The secretion of all the thermophilic enzymes [*Tf*Cut2, *TCur*0390, leaf and branch compost cutinase (LCC), and polyester hydrolase Leipzig 7 (PHL7)] was easily detected by the presence of clearance halos around producing colonies when cultured on plates containing the model substrate polycaprolactone (PCL), but not in the colonies expressing *Is*PETase or its variants (Figure 2A). We also tested the activity of the different enzymes against PET nanoparticles. However, clearance halos were detected only in colonies

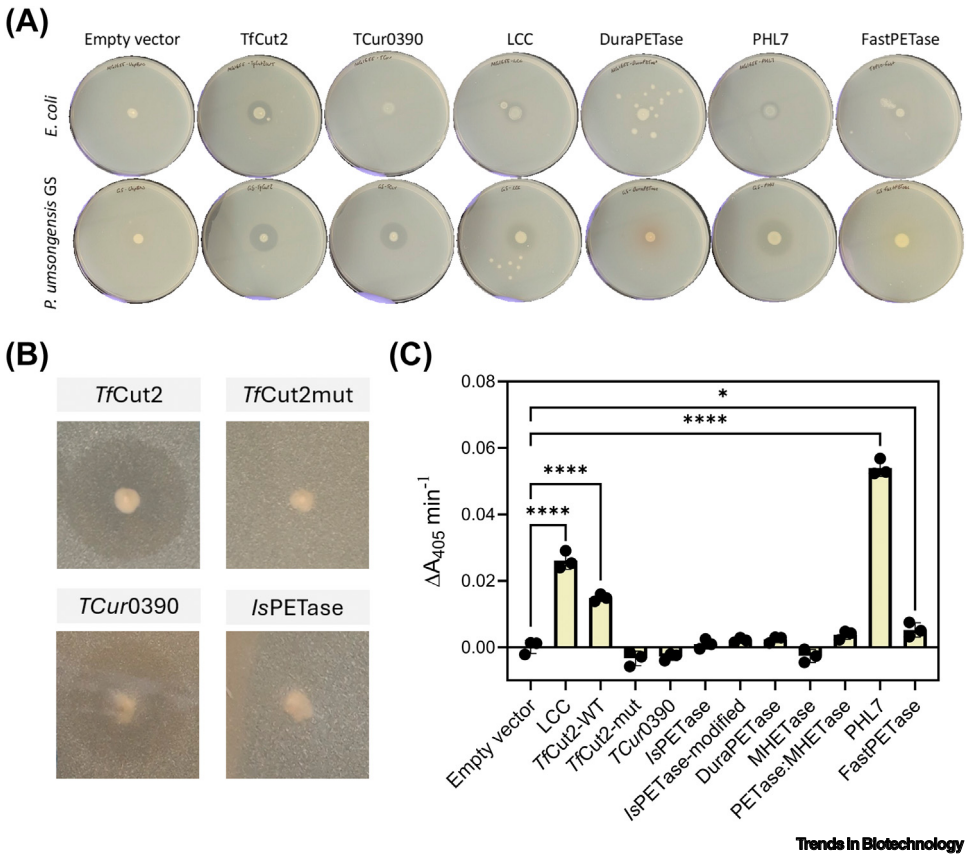

Figure 2. Activity of PET hydrolases recombinantly expressed and secreted. (A) PCL degradation assay on agar plates. (B) PET nanoparticle hydrolysis activity of selected enzymes expressed in *P. umsongensis* GS. (C) Activity of *E. coli* BL21 cell culture supernatants containing recombinantly expressed enzymes against *p*-nitrophenyl-butyrate (*p*NPB), measured as ΔA_{405} min^{-1} at 30°C. *Is*PETase modified refers to the W159H-S238F variant [39] (also refer to Figure S2A, B). Bars and error bars represent the mean and standard deviation, respectively, of three independent replicates. Significant differences within groups were determined by one-way analysis of variance (ANOVA) with post hoc Dunnett's test; significance thresholds are defined in the STAR Methods.

producing thermophilic enzymes after incubation at 50°C (Figure 2B), but not in the case of mesophilic enzymes (not shown) or in a negative control of *Tf*Cut2 (*Tf*Cut2mut) generated in this work, carrying the inactivating mutation S187A.

In the following experiment, we set out to identify the best enzyme to support microbial growth, which is expected to correlate with the total level of activity found in the culture supernatants of the bacteria. Levels of enzymatic activity using purified enzymes vary widely between publications, as there is no standardised method for measuring polyester depolymerisation activity since reaction conditions change from one study to another. To mitigate this problem, we conducted a side-by-side comparison of the activity of enzymes secreted into the culture broth by *E. coli* containing the different plasmids in a 48-hour culture. In these experiments, the activity determined is the result of a combination of several factors, including the kinetic properties of the enzyme in the culture medium and the ability of the strain to secrete a particular enzyme, all of which can vary for each enzyme; none of these properties were determined individually.

Under the conditions tested, PHL7 showed the greatest promise in supporting microbial growth on PET. Given the general lack of activity of *Is*PETase derivatives against PCL, we used the model substrate *p*-nitrophenyl butyrate (*p*NPB) to detect the presence of hydrolytic activity on ester bonds for all the enzymes in culture supernatants at different temperatures (Figure S2, in the Supplemental information online). In this assay, the presence of activity was detected by an increase in absorbance at 405 nm following the hydrolysis of the substrate *p*NPB, with kinetics at 30°C and 42°C shown in Figure S2A. Once again, supernatants containing the thermophilic enzymes all exhibited clear activity against the model substrate at 42°C (Figure S2B) and even at the lowest temperature of 30°C (Figure 2C), with the most apparent activity being observed for LCC and PHL7. A low activity against *p*NPB was detected for the mesophilic *Is*PETase derivative FastPETase, which has been engineered to be significantly more active than the WT version of the enzyme [40].

Solvent-pretreated PET shows high availability for enzymatic hydrolysis

Having confirmed the ability of the strains to secrete active PET hydrolases had been confirmed, we examined the use of different forms of PET as reaction substrates. We evaluated four amorphous PET materials, including commercial films, cryomilled PET, a sieved cryomilled microplastic fraction (<100 µm), and a solvent-pretreated (PT) amorphous macroporous material with a specific surface area of 45 m^2 g^{-1} (Figure 3A). The crystallinity of the polymer is a crucial property defining its degradability, and only amorphous PET can be efficiently hydrolysed enzymatically [44,45]. Differential scanning calorimetry (DSC) revealed no differences in crystallinity between the commercial amorphous film (6.91 ± 0.06%), cryomilled film (6.20 ± 0.08%), and the sieved cryomilled film microplastics (6.88 ± 0.47%), whereas the crystallinity was increased in the solvent-PT film material (17.90 ± 0.42%), as shown in Figure S3, in the Supplemental information online. The different PET substrates were incubated with culture supernatants from *E. coli* producing a selection of the enzymes in our collection. After 3 weeks of incubation at 30°C, the release of the PET monomer TA into the supernatant was determined by measuring absorbance at 240 nm (Figure 3B). The presence of TA in supernatant samples exceeding background absorbance was further confirmed by mass spectrometry (MS) (Figure 3C).

Under the conditions tested, enzymatic hydrolysis was detected exclusively for the solvent-PT PET, and among the enzymes evaluated, PHL7, FastPETase, and the MHETase–PETase chimera exhibited the highest activity, outperforming LCC. These enzymes released TA at concentrations in the millimolar range, consistent with levels required to sustain microbial growth. Together, these results identified PHL7 as the most promising hydrolase and solvent-PT PET as

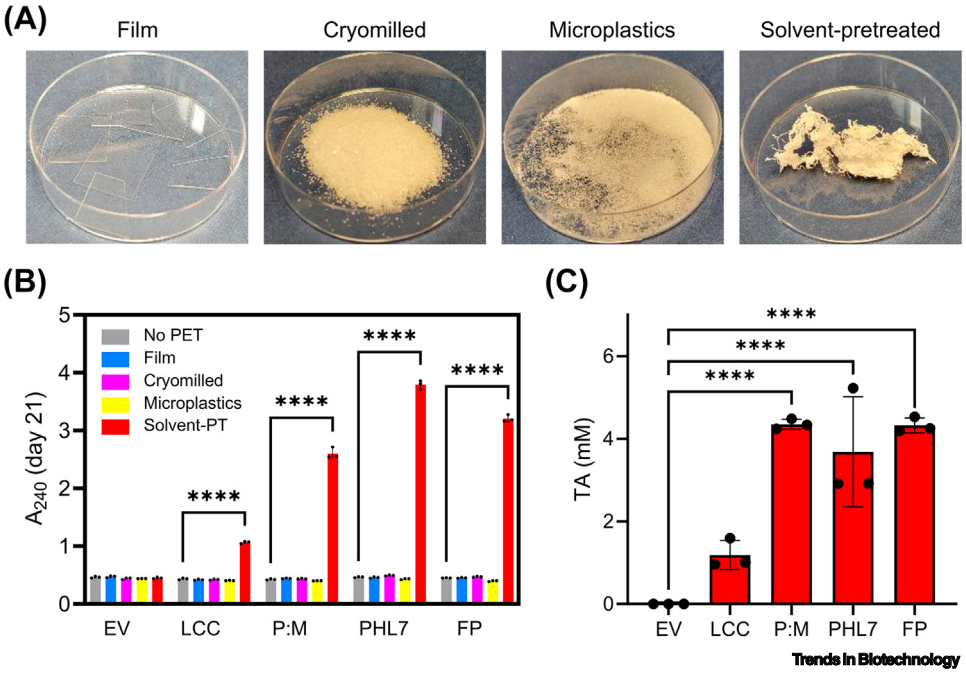

Figure 3. Effect of pretreatment on the availability of PET for enzymatic hydrolysis. (A) Images of PET substrates used: amorphous PET film (film; Goodfellow), cryomilled film (cryomilled), sieved cryomilled film using a 150-mesh sieve (microplastics), and solvent-pretreated film (solvent-PT) (also refer to Figure S3). (B) TA released from each PET substrate, monitored by A , following incubation at 30°C with *E. coli* BL21 cell culture supernatants containing the recombinantly expressed enzymes: leaf and branch compost cutinase (LCC), PETase:MHETase (P:M), PHL7, FastPETase (FP) and the empty pSEVA238 vector control (EV). (C) TA quantification by LC-MS in solvent- PT PET samples incubated with the same enzymes. Bars and error bars represent the mean and SEM, respectively, of three biological replicates. Significant differences within groups were determined by one-way ANOVA with post hoc Dunnett's test; significance thresholds are defined in the STAR Methods.

the most susceptible substrate, establishing the optimal combination for evaluating PET-supported microbial growth in *P. umsongensis* GS.

Utilisation of PET as a microbial feedstock

The results indicate that the combination of *P. umsongensis* GS as an expression host, PHL7 as the secreted hydrolase, and solvent-PT PET provides favourable conditions for PET-based growth. Therefore, to enable PET hydrolysis, we transformed strain GS with a plasmid encoding PHL7. Recombinant enzyme expression was optimised by varying inducer concentrations and quantifying esterase activity using a *p*NPB assay, with 0.5-mM inducer identified as optimal for subsequent experiments (Figure S4A, in the Supplemental information online).

Secretion of PHL7 into the culture supernatant was confirmed by SDS-PAGE analysis. A faint protein band was observed after 48 h in supernatants from the PHL7-expressing strain compared with samples taken at earlier timepoints, and a clear band was detected following concentration of the 48-h sample at the weight corresponding to that of the PHL7 protein control (27.6 kDa), consistent with the expected mass of PHL7 (27.8 kDa) (Figure S4B). Culture supernatants from both WT and PHL7-expressing strains, together with the excised concentrated band, were analysed by liquid chromatography-tandem mass spectrometry (LC-MS/MS), where PHL7 was confidently identified in the supernatant of the PHL7-expressing strain and in the excised gel band, with 14 out of 15 unique peptides detected (Uniprot accession A0AA82WPD4; Q-value

<0.001). No corresponding protein was detected in WT samples. Functional activity of the secreted enzyme was further demonstrated using bis(2-hydroxyethyl) terephthalate (BHET) agar plate assays, in which BHET served as a soluble PET degradation intermediate. Supernatants from the PHL7-expressing strain produced only minor visible changes compared with WT samples when tested directly (Figure S4C). However, upon concentration, clear halo zones were observed for the PHL7-expressing strain, indicating substrate hydrolysis, while no clearance was detected for WT supernatants (Figure S4D). These results confirm that PHL7 is secreted in an active form capable of hydrolysing PET-derived intermediates.

Subsequently, the ability of the engineered *P. umsongensis* GS to assimilate PET was evaluated by growing the isolate in minimal medium in the presence of PET and supplementing it with different concentrations of lysogeny broth (LB). This supplementation was required to support basal cellular metabolism and enzyme production, as no detectable growth or hydrolase expression was observed in the absence of LB. The need for additional carbon sources has also been reported in previous studies using organisms capable of PET degradation, such as *I. sakaiensis* [11] and *Comamonas testosteroni* [45].

In an initial experiment, the contribution of PET hydrolysis to growth was assessed by measuring the increase in optical density at 600 nm (OD_{600}) before and after 1 week of incubation at 30°C for strains producing PHL7 in the presence or absence of PT PET, alongside a corresponding empty plasmid control (Figure 4). The results show that TA alone did not enhance the growth of the control strain and was even detrimental under nutrient-rich conditions (Figure 4B). In contrast, when PHL7 was expressed, a significant growth difference between PHL7-producing and control cultures was observed in the presence of PET at the lowest LB concentration tested (10%) (p <0.0001) (Figure 4A). This difference diminished at higher LB concentrations, likely because the relative contribution of TA as a carbon source decreases as the medium becomes richer.

PET assimilation was further assessed by incubating *P. umsongensis* GS expressing PHL7 in the presence or absence of PET for 4 weeks. Under these conditions, cultures supplemented with PET showed an approximately twofold increase in biomass, consistent with utilisation of the plastic and increased cell viability over time (Figure 4C and Figure S4E). When the same experiment was conducted using the control strain *I. sakaiensis*, a similar qualitative trend was observed, with higher biomass in the presence of PET compared to PET-free controls. However, total biomass accumulation was approximately fourfold lower under identical M9 + 10% LB conditions (Figure 4D). Consistent with these observations, cell viability measurements showed that, compared to PHL7-producing *P. umsongensis* GS, *I. sakaiensis* maintained significantly lower colony-forming unit (CFU) ml^{-1} counts overall, with an initial increase in viability observed in M9 + 10% LB, possibly supported by LB supplementation, but this was not sustained during prolonged incubation (Figure S4F).

Taken together, these results indicate that PET hydrolysis contributes modestly but measurably to the growth of *P. umsongensis* GS expressing PHL7 and demonstrate that this engineered environmental bacterium can assimilate PET more efficiently than the naturally occurring PET-degrading strain tested under the same conditions.

Engineered bacteria can hydrolyse microplastics in WW

As mentioned in the introduction, one of the main advantages of **whole-cell catalysts** is their use in the bioremediation of plastics that are difficult to collect, such as microplastics. To evaluate whether engineered environmental bacteria could hydrolyse PET microplastics under

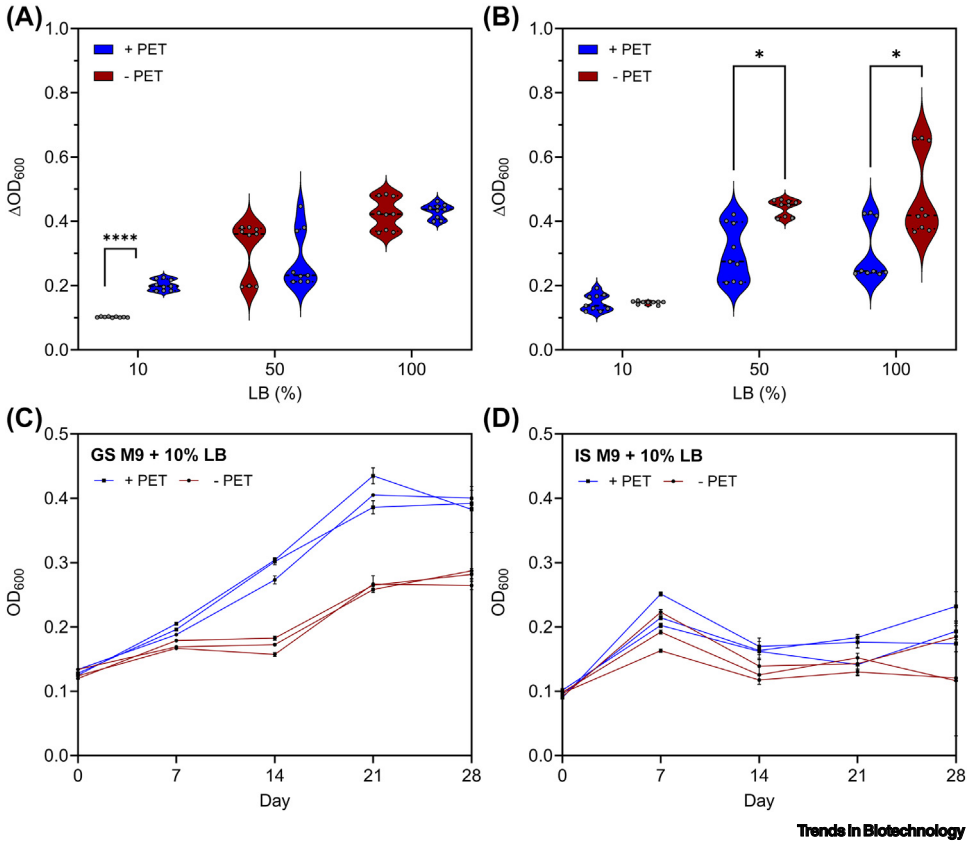

Figure 4. Growth of *P. umsongensis* GS expressing PHL7 using solvent-PT PET as a growth substrate. (A) Increase in optical density of *P. umsongensis* GS expressing PHL7 after 1 week of incubation in the presence (blue) or absence (red) of solvent-PT PET, with media supplemented with varying concentrations of LB. Statistical analysis is described in the Methods section (also refer to Figure S4A–D). (B) Growth of *P. umsongensis* GS carrying the empty plasmid pSEVA238 under the same conditions. Significant differences within groups were determined with a two-tailed t-test; significance thresholds are defined in the STAR Methods. (C) 4-week growth kinetics of *P. umsongensis* GS expressing PHL7 in the presence (blue) or absence (red) of solvent-PT PET. Lines represent individual trajectories from three independent cultures, each measured in triplicate, grown in M9 medium supplemented with 10% LB. (D) Growth kinetics of *I. sakaiensis* in M9 medium supplemented with 10% LB in the presence or absence of PET (also refer to Figure S4E,F).

environmentally relevant nonsterile conditions, degradation experiments were conducted using untreated WW collected from the water trap of an urban road gully as the reaction medium (Figure 5). Cryomilled PET microplastics (<100 μm) were suspended in WW and inoculated with either *P. umsongensis* GS expressing PHL7 or the corresponding WT strain. *I. sakaiensis* was included as a benchmark PET-degrading organism. All incubations were performed at 30°C with agitation, and samples were collected over 720 h for analysis of soluble PET-derived products.

In the GS WT condition, no measurable accumulation of mono(2-hydroxyethyl) terephthalate (MHET) was observed over the course of the experiment (Figure 5A). Instead, a BHET signal was detected at the initial timepoint, which declined over time, with only trace levels of terephthalic acid (TA) detected. The presence of BHET at 0 h suggests that soluble PET-associated oligomers were already present at the start of the assay, likely arising from leaching of the PT microplastic substrate rather than *de novo* biological depolymerisation. The subsequent decrease in BHET is consistent with turnover or removal of these compounds, potentially

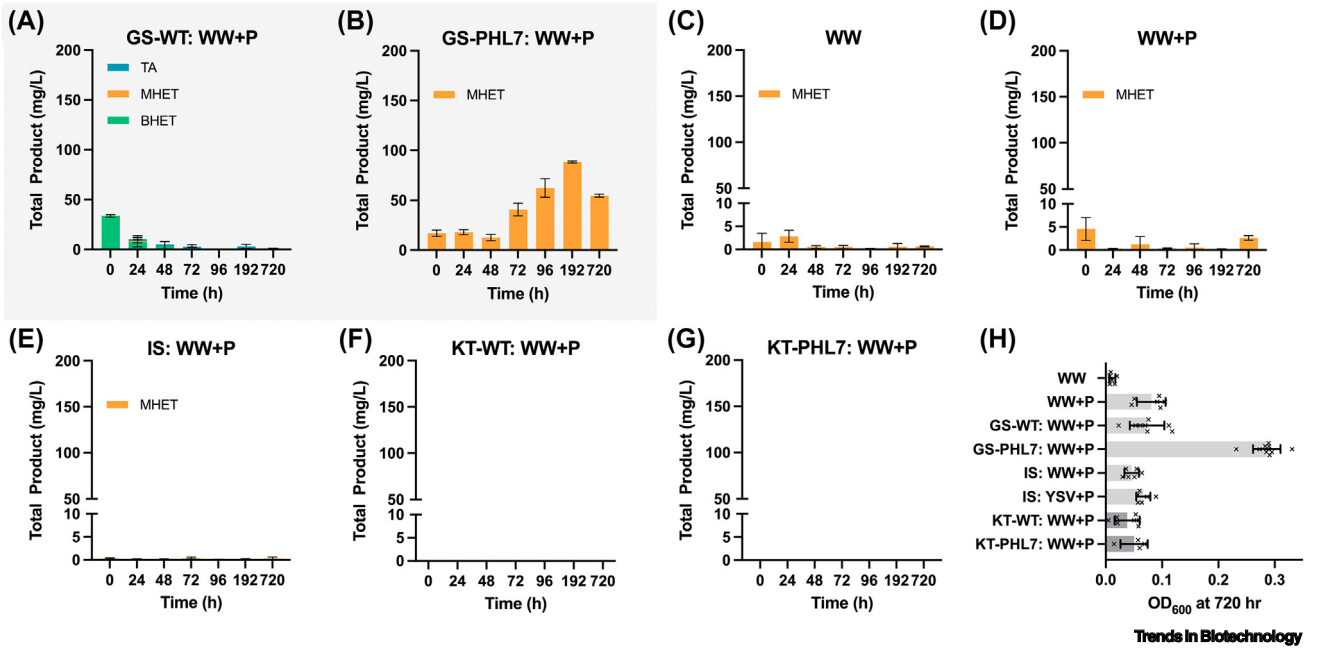

Figure 5. Growth and PET microplastic transformation under environmentally relevant wastewater (WW) conditions. (A–G) Time-course quantification of soluble PET-derived products and H endpoint biomass at 720 h in WW inoculated with PET (P). (A) WW alone (WW), (B) WW with PET microplastics (WW + P). (C–D) *P. umsongensis* GS (GS) analysis in WW + P (grey panels): (C) GS wild type (GS-WT) and (D) GS expressing PHL7 (GS-PHL7). (E) WW + P inoculated with *I. sakaiensis*. (F–G) *P. putida* KT2440 (KT) analysis in WW + P: (F) KT2440 wild type (KT-WT) and (G) KT2440 expressing PHL7 (KT-PHL7). Product formation is shown as BHET (green), MHET (orange), and TA (blue), with the y-axis representing total product concentration (mg/l). Samples were collected every 24 h up to 96 h, with additional timepoints at 192 h and 720 h. All experiments were performed in 2 ml WW containing 10 mg PET microplastic (where indicated) at 30°C with shaking at 300 rpm. (H) Endpoint OD_{600} measurements at 720 h for all conditions and YSV + P inoculated with *I. sakaiensis* (Figure S5). Data represent biological triplicates with standard deviation shown as error bars. Significant differences within groups were determined by one-way ANOVA with post hoc Dunnett's test; significance thresholds are defined in the STAR Methods.

mediated by the native microbial community present in the WW, rather than sustained PET hydrolysis by the WT strain.

In contrast, the PHL7-expressing GS strain exhibited clear accumulation of MHET over time in WW containing PET microplastics (Figure 5B). MHET concentrations increased progressively, reaching a maximum of 88.45 mg l^{-1} total product release at approximately 192 h before declining slightly at 720 h, suggesting that MHET is both produced and subsequently subject to downstream transformation or consumption. This accumulation profile was not observed in any control condition, indicating that the heterologous expression of PHL7 enabled PET depolymerisation under these environmental conditions and shifted the detectable product profile towards MHET as the dominant soluble intermediate. In WW-only controls, low but detectable MHET signals were observed, including early timepoint peaks in both WW and WW + PET conditions (Figure 5C,D), indicating that the environmental matrix is not analytically inert and may contribute background signal or low-level transformation of PET-derived material.

Under the same conditions, *I. sakaiensis* showed only limited accumulation of soluble intermediates in WW (Figure 5E), despite its reported PET-degrading capability. This suggests that extracellular product accumulation is constrained in this complex environmental matrix, potentially due to rapid uptake or metabolism of intermediates by the surrounding microbial community. Control conditions further contextualised these observations, where in the defined medium yeast

extract-sodium carbonate-vitamins (YSV), optimal for *I. sakaiensis* growth, MHET accumulation was negligible in the absence of cells (Figure S5A, in the Supplemental information online), and in YSV supplemented with PET (YSV + P), only very low levels of MHET were detected, primarily at later timepoints (192 and 720 h), consistent with slow abiotic release or low-level microbial turnover of PET-derived intermediates (Figure S5B). Upon inoculation with *I. sakaiensis* (YSV + P + IS), MHET levels returned to negligible, suggesting rapid uptake or further metabolism of any released products (Figure S5C).

Across all conditions except the PHL7-expressing strain, MHET was the only consistently detected PET-derived intermediate, while BHET and TA were largely absent or detected only transiently. The limited detection of TA likely reflects rapid uptake and metabolism by the native microbial community present in the WW matrix, preventing extracellular accumulation. Similarly, the general absence of sustained BHET accumulation is consistent with the reported activity and mechanism of PHL7, which primarily generates MHET as the initial hydrolysis product, which is then later hydrolysed into TA EG [42,46]. Together, these observations indicate that product accumulation in this system reflects a balance between depolymerisation, transformation, and consumption processes occurring within a complex environmental microbial community.

We further tested this by using *P. putida* KT2440 WT and a PHL7-expressing strain as controls (Figure 5F,G). Both are unable to assimilate the resulting monomers, including the strain expressing a PET hydrolase, and no hydrolysis products were detected. Endpoint biomass measurements further supported these findings (Figure 5H). OD_{600} at 720 h was highest in cultures of GS expressing PHL7 in WW with PET, reaching approximately 0.3. In contrast, all other conditions, including *I. sakaiensis* and the GS WT strain, remained markedly lower (~0.1). Importantly, growth was observed in WW with PET but not in WW alone, consistent with the presence of a native microbial community capable of utilising PET-derived compounds. Concurrent with the lack of MHET detection, the KT2440 controls did not show any biomass accumulation. The increased biomass observed for the PHL7-expressing strain is therefore consistent with greater availability of utilisable carbon derived from PET hydrolysis. Taken together, these results show that PHL7-mediated depolymerisation enhances growth in organisms capable of assimilating PET monomers, suggesting that PET-trophy can be leveraged for improved microplastic biodegradation.

Discussion

In this work, we demonstrate the feasibility of using a whole-cell catalyst directly after its isolation in an environmental screening for the direct assimilation of PET waste plastic under mesophilic conditions. This required combining efficient secretion of highly active PET-degrading enzymes with a host naturally capable of metabolising TA, together with the use of PET substrates PT to increase susceptibility to hydrolysis.

Enzymatic depolymerisation of PET remained the principal limiting step in the process. In contrast, isolating organisms capable of mineralising TA and amenable to genetic manipulation proved comparatively straightforward. We identified two strains of *P. umsongensis*, a species previously shown to upcycle TA into the bioplastic polyhydroxyalkanoate [47]. However, identifying an enzyme capable of supporting sustained bacterial growth on PET remains a bottleneck both in this study and in the broader field [28]. To address this limitation, we evaluated several PET hydrolases reported to date, including enzymes from both mesophilic and thermophilic organisms.

Thermophilic enzymes have consistently demonstrated higher activity than their mesophilic counterparts, many of which are derived from *Is*PETase [48]. This increased activity at elevated

temperatures is generally attributed to enhanced polymer chain mobility as PET approaches its glass transition temperature (T_g ~ 70°C). However, such temperatures are incompatible with the optimal growth conditions required for most biotechnologically relevant microorganisms. Notably, our results show that thermophilic enzymes, such as *Tf*Cut2 and PHL7 present in culture supernatants, can still outperform *Is*PETase and its variants, including FP, at lower temperatures. Among all enzymes tested, PHL7 exhibited the highest activity against PET and the model substrates PCL and *p*NPB, including when reactions were performed directly in cell culture medium. Previous work indicates that PHL7 activity depends on high phosphate concentrations (1 M) [42], and therefore its robust performance here may reflect compatibility with the phosphate-rich M9 (0.35 mM phosphate) media used [49]. The amount of TA released from PET under these conditions was in the low millimolar range, consistent with the observed biomass increase of the engineered strain, corresponding to approximately half the biomass obtained when 10 mM TA was supplied directly.

The comparison with the natural PET degrader *I. sakaiensis* provides a direct benchmark for evaluating the performance of the engineered *P. umsongensis* GS strain. Although both organisms showed increased biomass in the presence of PET, the engineered strain consistently achieved substantially higher biomass accumulation and maintained greater cell viability under identical cultivation conditions. Notably, biomass levels of *I. sakaiensis* remained markedly lower even in media conditions previously reported to support its growth, and cell viability declined over extended incubation. In contrast, the engineered GS strain sustained higher viable cell numbers throughout the experiment, suggesting that PET-derived carbon was more effectively incorporated into cellular metabolism. These differences may reflect not only enzymatic PET hydrolysis capacity but also broader physiological traits of the host organism, including substrate uptake, stress tolerance, and metabolic flexibility. The data, therefore, indicate that successful PET utilisation depends on both depolymerisation efficiency and the host cellular context in which this activity occurs. Together, these findings suggest that engineering robust environmental bacteria to express efficient PET-hydrolysing enzymes can outperform naturally occurring PET degraders under laboratory conditions, highlighting the potential of host optimisation as a critical design principle for future plastic bioconversion strategies.

We further showed that solvent-PT PET resulted in substantially higher hydrolysis rates compared to the same material subjected to alternative pretreatments, such as cryomilling. Our findings, together with previous reports [50], indicate that although solvent treatment can increase crystallinity, it also enhances polymer porosity, facilitating enzyme access. While solvent-based treatments present challenges for *in situ* bioremediation, they could be advantageous for collected PET waste streams, including textile recycling, where dye removal is an additional benefit [50]. Moreover, solvents such as γ-valerolactone can be produced from renewable feedstocks [51] and exhibit low toxicity [52], supporting broader industrial applicability. Cryomilling, although commonly used, is energy intensive and contributes significantly to process costs. Solvent-based approaches offer lower-energy alternatives with potential for solvent recovery and reuse [53]. In addition to sustainability considerations, technoeconomic analyses have shown that energy costs associated with pretreatment and enzyme production strongly influence the competitiveness of enzymatic recycling relative to virgin PET production [54]. In this context, combining low-energy pretreatment with *in situ* enzyme production and conversion to value-added products could offer a viable approach for PET waste streams that are difficult to collect [55,56].

Environmental simulations provided insight into the performance of engineered PET-degrading systems in complex, nonsterile environments. In untreated WW, soluble product accumulation

was dominated by MHET, with little to no sustained detection of BHET or TA, indicating that intermediate turnover and microbial consumption strongly influence observable product profiles. The presence of low background signals in control conditions further demonstrates that environmental matrices are not inert but instead contain pre-existing compounds and active microbial processes that can both generate and remove PET-derived intermediates. As a result, extracellular product accumulation reflects a dynamic balance between enzymatic depolymerisation and rapid downstream utilisation, rather than a simple readout of hydrolytic activity. The presence of bioavailable growth substrates in runoff WW samples has been widely characterised in the literature. In particular, urban gully pots contain a diverse set of organic chemicals both in solution and in sediments [57,58], which include, among others, aliphatic, monoaromatic, and humic acid-like molecules [59]. Some of these molecules can be readily metabolised by microorganisms during water treatment processes to reduce dissolved organic content prior to the release of effluents [60]. The concentration of this readily bioavailable fraction is typically reported as the 5-day biological oxygen demand (BOD5), which is defined as the amount of dissolved oxygen microorganisms consume while breaking down biodegradable organic matter in a water sample over a five-day period at 20°C [61]. Runoff stormwaters, like the samples used, can contain widely varied BOD5 levels ranging from 0.1 to 430 mg/l [62], with models for urban road environments reporting peak BOD5 values of 98–137 mg/l [63]. For reference, the BOD standard solution containing 150 mg/l glucose and 150 mg/l glutamic acid has a BOD5 of 198 mg/l [61,64]. Considering that the upper end of this BOD range (98–137 mg/l) is roughly equivalent to one-tenth of the substrate used in standard laboratory growth experiments, it is therefore unsurprising that the WW samples used supported initial microbial growth, which becomes self-sustained once enough PET hydrolase accumulates in the suspension.

Within this context, the engineered GS strain expressing PHL7 enabled measurable PET depolymerisation in WW, as evidenced by the accumulation of MHET over time, whereas the WT strain showed no such activity. The limited accumulation of downstream products such as TA is consistent with rapid uptake by the native microbial community, highlighting that product profiles in environmental systems reflect a balance between depolymerisation and microbial consumption, rather than simple accumulation of degradation products.

Interestingly, PET microplastic hydrolysis by PHL7 was not observed in the cell-free *E. coli* supernatant assay (Figure 3) yet it was detectable in the WW system using the live *Pseudomonas* host (Figure 5). This difference likely reflects the distinct experimental contexts, including sustained enzyme production in the live host and interactions with the environmental matrix. These findings emphasise that enzyme performance in simplified, cell-free assays may underestimate activity under more complex, environmentally relevant conditions.

Additionally, the relatively low hydrolysis rates observed highlight the continued need for enzyme engineering to improve activity at the solid–liquid interface of post-consumer PET. This will require screening strategies beyond conventional colorimetric assays using soluble model substrates, which often fail to capture the complexity of enzyme-polymer interactions in heterogeneous materials. Alternative approaches, such as impedance spectroscopy [65], which enables real-time monitoring of plastic degradation, may provide more relevant screening platforms. Another promising strategy is the development of thermophilic whole-cell catalysts capable of operating closer to PET's T_g, as demonstrated by engineering *Clostridium thermocellum* to express LCC [66]. In addition, aerobic aromatic assimilation pathways, including the ketoadipate pathway for protocatechuate assimilation, are also present in thermophilic *Geobacillus* species [67], suggesting potential for thermophilic PET-assimilating systems. Beyond enzymatic activity, our results also highlight additional rate-limiting steps in the pipeline, including enzyme production and secretion, that remain amenable to optimisation.

Furthermore, the assimilation of hydrolysis products such as TA and EG could be further improved through adaptive laboratory evolution, which has been successfully applied to enhance monomer uptake and co-utilisation in *P. putida* [30].

Concluding remarks

The modular pipeline developed in this study demonstrates that active PET hydrolases can be expressed and secreted in diverse microbial hosts. Even with modest hydrolysis rates, whole-cell catalysts influenced PET transformation dynamics under environmentally relevant conditions during multiday incubations. The accumulation of MHET and increased biomass suggests that engineered depolymerisation contributes to carbon availability, although further work is required to quantify net PET degradation and the role of native microbial communities. However, deploying engineered organisms in open environments presents regulatory and biosafety challenges that must be addressed before real-world applications. Current regulations generally prohibit the release of genetically modified organisms outside confined settings, though limited exemptions exist under specific regulatory frameworks, such as in the UK [68]. Consequently, engineered strains intended for environmental applications would need to incorporate robust biocontainment strategies, such as kill-switch mechanisms or auxotrophic dependencies, to prevent uncontrolled proliferation and unintended ecological impacts [69]. In WW treatment contexts, thermal hydrolysis steps commonly applied to sludge processing may partly mitigate such concerns by sterilising biomass prior to environmental release.

Although the engineered microorganisms described here exhibit only modest growth on PET, this work establishes a foundation for further optimisation. The study highlights current bottlenecks in whole-cell PET hydrolysis and assimilation while identifying opportunities for improvement (see Outstanding questions). Beyond degradation itself, PET-dependent growth could enable growth-coupled screening and directed evolution of improved PET hydrolases. Direct selection based on cellular fitness would accelerate laboratory evolution of whole-cell catalysts and promote more efficient PET degradation by linking polymer hydrolysis to cellular growth, thereby sustaining enzyme production without continuous external induction or supplementation. This would advance efforts towards bioremediating and upcycling persistent plastic waste into value-added products. In contrast to nonassimilative degraders, assimilating microbes could self-propagate on heterogeneous PET waste streams, improving robustness, process stability, and long-term efficiency in open or low-control environments.

STAR★METHODS

Detailed methods are provided in the online version of this paper and include the following:

- Key resources table
- EXPERIMENTAL MODEL AND STUDY PARTICIPANT DETAILS
  - Strain isolation
  - Whole-genome sequencing and analysis
  - Microbial culturing
- METHOD DETAILS
  - PET pretreatment
  - Polymer differential scanning calorimetry
  - Plasmid assembly and strain engineering
  - Esterase enzymatic assays and TA determination
  - PHL7 expression optimisation
  - PHL7 proteomic determination
  - PHL7 polyacrylamide gel electrophoresis (PAGE) and activity assays

Outstanding questions

Can plastics become effective microbial feedstocks, similar to biodegradable polymers?

Is large-scale application in wastewater treatment plants of poly (ethylene terephthalate) (PET)-degrading bacteria possible with current PET degradation rates?

Can rational engineering or directed evolution increase the biodegradation rates of PET?

Can highly crystalline PET microplastics be biodegraded?

Can microplastics other than polyesters and polyamides be reliably degraded by microorganisms?

- Environmental wastewater PET microplastic degradation
- Violacein determination
- QUANTIFICATION AND STATISTICAL ANALYSIS

Resource availability

Lead contact

Requests for further information and resources should be directed to, and will be fulfilled by, the lead contact, Dr José Jiménez (j.jimenez@imperial.ac.uk).

Materials availability

Strains and plasmids generated in this study will be made available upon request, but we may require a payment and/or a completed materials transfer agreement if there is potential for commercial application.

Data and code availability

The genomic sequences of the environmental isolates have been deposited in the NIH's GenBank with accession number PRJNA831356 and are publicly available as of the date of publication. All data shown in the figures of this research article will be made available by the lead contact upon request after publication. This research article does not report original code. Any additional information required to reanalyse the data reported in this research article is available from the lead contact upon request.

Author contributions

A.M.B., U.A., B.W., P.P., C.A.R., W.Z., and J.I.J. conceived and designed the research. A.M.B., U.A., B.W., C.S., H.D., Z.Z., J.K., C.B., S.B., R.W., C.A.O., G.L.M., and J.I.J. carried out the experiments and respective analyses. All authors wrote and edited the manuscript.

Acknowledgements

The authors are indebted to Dr Tom Bond (University of Surrey, UK) for his support in producing cryomilled PET. The authors acknowledge the Proteomics Facility and Dr Jianan Lu at the Molecular Sciences Research Hub, Department of Chemistry, Imperial College London, for their support with LC-MS/MS acquisition and data analysis. The authors also acknowledge the Centre for Enzyme Innovation, School of the Environment and Life Sciences, University of Portsmouth, for providing access to HPLC and DSC instrumentation. The authors acknowledge the support received from the Biotechnology and Biological Sciences Research Council (BBSRC) through the grants BB/Y007972/1 as well as BB/T011289/2, and from the Sächsisches Staatsministerium für Wissenschaft, Kultur und Tourismus (Project no. 100387903), sponsored as part of the ERA-CoBiotech project MIPLACE. The authors would also like to acknowledge the support received from the European Union's Horizon 2020 research and innovation programme under grant agreement no. 633962 for the project P4SB. U.A. was the recipient of a PhD studentship from the Petroleum Technology Development Fund of Nigeria. The vector symbols corresponding to a bottle and a plant used in the graphical abstract were designed by jemastock and brgfx/Freepik, respectively, and downloaded from Magnific's library.

Declaration of interests

The authors, C.S. and W.Z., of Leipzig University declare that they have filed a patent related to the process for preparing the solvent-PT PET used in this study.

Declaration of Generative AI and AI-assisted technologies in the writing process

During the preparation of this work, the authors used Microsoft's Copilot in order to improve the readability and conciseness of specific parts of the abstract and discussion. The authors reviewed and edited the content as needed and take full responsibility for the content of the publication.

Supplemental information

Supplementary information associated with this article can be found online at https://doi.org/10.1016/j.tibtech.2026.06.008.

References

1. Barnes, D.K.A. *et al.* (2009) Accumulation and fragmentation of plastic debris in global environments. *Philos. Trans. R. Soc. B Biol. Sci.* 364, 1985–1998
2. Park, S.H. and Kim, S.H. (2014) Poly (ethylene terephthalate) recycling for high value added textiles. *Fash. Text.* 1, 1
3. Brivio, L. and Tollini, F. (2022) Chapter Six - PET recycling: review of the current available technologies and industrial perspectives. In *Towards Circular Economy: Closing the Loop with Chemical Recycling of Solid Plastic Waste* (Vol. 60) (Moscatelli, D. and Pelucchi, M., eds), pp. 215–267, Academic Press
4. Liu, C. *et al.* (2019) Widespread distribution of PET and PC microplastics in dust in urban China and their estimated human exposure. *Environ. Int.* 128, 116–124
5. Corradini, F. *et al.* (2019) Evidence of microplastic accumulation in agricultural soils from sewage sludge disposal. *Sci. Total Environ.* 671, 411–420
6. Vasse, G.F. and Melgert, B.N. (2024) Microplastic and plastic pollution: impact on respiratory disease and health. *Eur. Respir. Rev.* 33, 230226
7. Maurya, A. *et al.* (2020) Enzymatic remediation of polyethylene terephthalate (PET)-based polymers for effective management of plastic wastes: an overview. *Front. Bioeng. Biotechnol.* 8, 602325
8. García, J.L. (2022) Enzymatic recycling of polyethylene terephthalate through the lens of proprietary processes. *Microb. Biotechnol.* 15, 2699–2704
9. Roth, C. *et al.* (2014) Structural and functional studies on a thermostable polyethylene terephthalate degrading hydrolase from *Thermobifida fusca*. *Appl. Microbiol. Biotechnol.* 98, 7815–7823
10. Wei, R. *et al.* (2014) Functional characterization and structural modeling of synthetic polyester-degrading hydrolases from *thermomonospora curvata*. *AMB Express* 4, 44
11. Yoshida, S. *et al.* (2016) A bacterium that degrades and assimilates poly(ethylene terephthalate). *Science* 351, 1196–1199
12. Wierckx, N. *et al.* (2019) Plastic Biodegradation: challenges and opportunities. In *Consequences of Microbial Interactions with Hydrocarbons, Oils, and Lipids: Biodegradation and Bioremediation* (Steffan, R.J., ed.), pp. 333–361, Springer International Publishing
13. Johnson, N.W. *et al.* (2025) A biocompatible lossen rearrangement in *Escherichia coli*. *Nat. Chem.* 17, 1020–1026
14. Royer, B. *et al.* (2026) Microbial upcycling of plastic waste to levodopa. *Nat. Sustainability* 9, 706–713
15. Wierckx, N. *et al.* (2015) Plastic waste as a novel substrate for industrial biotechnology. *Microb. Biotechnol.* 8, 900–903
16. Bayer, T. *et al.* (2022) Biosensor and chemo-enzymatic one-pot cascade applications to detect and transform PET-derived terephthalic acid in living cells. *iScience* 25, 104326
17. Sadler, J.C. and Wallace, S. (2021) Microbial synthesis of vanillin from waste poly(ethylene terephthalate). *Green Chem.* 23, 4665–4672
18. Fujiwara, R. *et al.* (2021) Direct fermentative conversion of poly (ethylene terephthalate) into poly(hydroxyalkanoate) by *Ideonella sakaiensis*. *Sci. Rep.* 11, 19991
19. Tiso, T. *et al.* (2021) Towards bio-upcycling of polyethylene terephthalate. *Metab. Eng.* 66, 167–178
20. Lee, E.S. *et al.* (2026) Metabolic engineering of *Pseudomonas putida* KT2440 for valorization of terephthalic acid to produce catechol and muconic acid. *New Biotechnol.* 93, 226–233
21. Wei, R. *et al.* (2025) Standardization guidelines and future trends for PET hydrolase research. *Nat. Commun.* 16, 4684
22. Uekert, T. *et al.* (2022) Life cycle assessment of enzymatic poly (ethylene terephthalate) recycling. *Green Chem.* 24, 6531–6543
23. Jiménez, J.I. *et al.* (2026) Engineering whole-cell catalysts to use plastic waste as a feedstock. *Curr. Opin. Biotechnol.* 97, 103443
24. Benton, J. *et al.* (2026) Reflections on bio-based PET and plastic waste management: a responsible research and innovation approach. *Nat. Commun.* 17, 2281
25. Benton, J. *et al.* (2024) *Using microbes to remove microplastics from wastewater and sewage sludge, Institute of Molecular Science and Engineering*.
26. Liu, F. *et al.* (2025) Efficient biodegradation and upcycling of polyethylene terephthalate mediated by cell-factories. *Front. Microbiol.* 16, 16–2025
27. Lai, Y. *et al.* (2026) A strategy for *in situ* sustainable PET degradation in soil by genetically engineered bacteria constructed from indigenous strains. *J. Hazard. Mater.* 508, 141882
28. Brandenberg, O.F. *et al.* (2022) Towards synthetic PETtrophy: engineering *Pseudomonas putida* for concurrent polyethylene terephthalate (PET) monomer metabolism and PET hydrolase expression. *Microb. Cell Factories* 21, 119
29. Seo, H. *et al.* (2019) Production of extracellular PETase from *Ideonella sakaiensis* using sec-dependent signal peptides in *E. coli*. *Biochem. Biophys. Res. Commun.* 508, 250–255
30. Werner, A.Z. *et al.* (2025) Adaptive laboratory evolution and genetic engineering improved terephthalate utilization in *Pseudomonas putida* KT2440. *Metab. Eng.* 88, 196–205
31. Liu, P. *et al.* (2022) Valorization of polyethylene terephthalate to muconic acid by engineering *pseudomonas putida*. *Int. J. Mol. Sci.* 23, 10997
32. Mikio, S. *et al.* (2006) Characterization of the terephthalate degradation genes of Comamonas sp. strain E6. *Appl. Environ. Microbiol.* 72, 1825–1832
33. Elbehiry, A. *et al.* (2022) Pseudomonas species prevalence, protein analysis, and antibiotic resistance: an evolving public health challenge. *AMB Express* 12, 53
34. Durán, N. *et al.* (2016) Advances in Chromobacterium violaceum and properties of violacein—its main secondary metabolite: a review. *Biotechnol. Adv.* 34, 1030–1045
35. Molpeceres-García, F.J. *et al.* (2026) *Pseudomonas putida* JM37 as a novel bacterial chassis for ethylene glycol upcycling. *Bioresour. Technol.* 443, 133884
36. Darlington, A.P.S. *et al.* (2018) Dynamic allocation of orthogonal ribosomes facilitates uncoupling of co-expressed genes. *Nat. Commun.* 9, 695
37. Wei, R. *et al.* (2022) Mechanism-based design of efficient PET hydrolases. *ACS Catal.* 12, 3382–3396
38. Austin, H.P. *et al.* (2018) Characterization and engineering of a plastic-degrading aromatic polyesterase. *Proc. Natl. Acad. Sci. U. S. A.* 115, E4350–E4357
39. Lu, H. *et al.* (2022) Machine learning-aided engineering of hydrolases for PET depolymerization. *Nature* 604, 662–667
40. Cui, Y. *et al.* (2021) Computational redesign of a PETase for plastic biodegradation under ambient condition by the GRAPE strategy. *ACS Catal.* 11, 1340–1350
41. Sintawee, S. *et al.* (2012) Isolation of a novel cutinase homolog with polyethylene terephthalate-degrading activity from leaf-branch compost by using a metagenomic approach. *Appl. Environ. Microbiol.* 78, 1556–1562
42. Sonnendecker, C. *et al.* (2022) Low carbon footprint recycling of post-consumer PET plastic with a metagenomic polyester hydrolase. *ChemSusChem* 15, e202101062
43. Putker, F. *et al.* (2013) The type II secretion system (Xcp) of *Pseudomonas putida* is active and involved in the secretion of phosphatases. *Environ. Microbiol.* 15, 2658–2671
44. Ronkvist, Å.M. *et al.* (2009) Cutinase-catalyzed hydrolysis of poly (ethylene terephthalate). *Macromolecules* 42, 5128–5138
45. Wilkes, R.A. *et al.* (2024) Mechanisms of polyethylene terephthalate pellet fragmentation into nanoplastics and assimilable carbons by wastewater *Comamonas*. *Environ. Sci. Technol.* 58, 19338–19352
46. Richter, P.K. *et al.* (2023) Structure and function of the metagenomic plastic-degrading polyester hydrolase PHL7 bound to its product. *Nat. Commun.* 14, 1905
47. Narancic, T. *et al.* (2021) Genome analysis of the metabolically versatile *Pseudomonas umsongensis* GO16: the genetic basis for PET monomer upcycling into polyhydroxyalkanoates. *Microb. Biotechnol.* 14, 2463–2480
48. Kawai, F. (2021) The current state of research on PET hydrolyzing enzymes available for biorecycling. *Catalysts* 11, 206
49. Cold Spring Harbor Laboratory (2010) M9 minimal medium (standard). *Cold Spring Harb Protoc* 2010 pdb.rec12295
50. Wain, B. *et al.* (2026) Is solvent-based dissolution and precipitation an effective substrate pretreatment for the enzymatic depolymerisation of poly(ethylene terephthalate)? *Faraday Discuss.* 262, 367–384

51. Chen, W. *et al.* (2021) Biomass-derived γ-valerolactone: efficient dissolution and accelerated alkaline hydrolysis of polyethylene terephthalate. *Green Chem.* 23, 4065–4073
52. Kerkel, F. *et al.* (2021) The green platform molecule gamma-valerolactone – ecotoxicity, biodegradability, solvent properties, and potential applications. *Green Chem.* 23, 2962–2976
53. Tonsi, G. *et al.* (2025) The selective dissolution-precipitation recycling: a review on this alternative approach for the recovery of nylon-based waste materials. *Waste Manag.* 204, 114937
54. Singh, A. *et al.* (2021) Techno-economic, life-cycle, and socio-economic impact analysis of enzymatic recycling of poly(ethylene terephthalate). *Joule* 5, 2479–2503
55. Wei, Z. *et al.* (2024) Resource recovery of high value-added products from wastewater: current status and prospects. *Bioresour. Technol.* 398, 130521
56. Mannina, G. *et al.* (2020) Recovery of polyhydroxyalkanoates (PHAs) from wastewater: a review. *Bioresour. Technol.* 297, 122478
57. Wei, H. *et al.* (2023) A study of 101 organic substances in gully pot sediments accumulated over a one-year period in Stockholm, Sweden. *Sci. Total Environ.* 894, 165028
58. Wei, H. *et al.* (2024) Impacts of seasonal activities and traffic conditions on the contamination and accumulation of gully pot sediments: metal(loid)s and organic substances. *Sci. Total Environ.* 948, 174749
59. Niu, S. *et al.* (2024) Occurrence of dissolved organic matter in storm-drain inlet sediments and its implication for urban stormwater infrastructure sustainability. *Resour. Environ. Sustain.* 16, 100158
60. Du, X. *et al.* (2024) Removal of dissolved organic matter in road runoff with sludge-based filters from the drinking water treatment plant. *Water Sci. Technol.* 91, 160–173
61. Eaton, A.D. *et al.* (1995) *Standard Methods for the Examination of Water and Wastewater*, American Public Health Association
62. Pamuru, S.T. *et al.* (2022) Chemical characterization of urban stormwater: traditional and emerging contaminants. *Sci. Total Environ.* 813, 151887
63. Hur, S. *et al.* (2018) Development of urban runoff model FFC-QUAL for first-flush water-quality analysis in urban drainage basins. *J. Environ. Manag.* 205, 73–84
64. Pasco, N. *et al.* (2000) Biochemical mediator demand – a novel rapid alternative for measuring biochemical oxygen demand. *Appl. Microbiol. Biotechnol.* 53, 613–618
65. Frank, R. *et al.* (2022) Real-time noninvasive analysis of biocatalytic PET degradation. *ACS Catal.* 12, 25–35
66. Yan, F. *et al.* (2021) Thermophilic whole-cell degradation of polyethylene terephthalate using engineered clostridium thermocellum. *Microb. Biotechnol.* 14, 374–385
67. Bubinas, A. *et al.* (2008) Degradation of naphthalene by thermophilic bacteria via a pathway, through protocatechuic acid. *Cent. Eur. J. Biol.* 3, 61–68
68. UK Government (2002) *Genetically Modified Organisms (Deliberate Release) Regulations 2002*, The Stationery Office
69. George, D.R. *et al.* (2024) A bumpy road ahead for genetic biocontainment. *Nat. Commun.* 15, 650
70. Bolger, A.M. *et al.* (2014) Trimmomatic: a flexible trimmer for Illumina sequence data. *Bioinformatics* 30, 2114–2120
71. Bankevich, A. *et al.* (2012) SPAdes: a new genome assembly algorithm and its applications to single-cell sequencing. *J. Comput. Biol.* 19, 455–477
72. Seemann, T. (2014) Prokka: rapid prokaryotic genome annotation. *Bioinformatics* 30, 2068–2069
73. Silva-Rocha, R. *et al.* (2013) The Standard European Vector Architecture (SEVA): a coherent platform for the analysis and deployment of complex prokaryotic phenotypes. *Nucleic Acids Res.* 41, D666–D675
74. Malke, H. (1990) J. SAMBROCK, E. F. FRITSCH and T. MANIATIS, molecular cloning, a laboratory manual (second edition), volumes 1, 2, and 3. 1625S., zahlreiche Abb. und Tab. Cold Spring Harbor 1989. cold spring harbor laboratory press. $ 115.00. ISBN: 0-87969-309-6. *J. Basic Microbiol.* 30, 623
75. Blattner, F.R. *et al.* (1997) The complete genome sequence of *Escherichia coli* K-12. *Science* 277, 1453–1462
76. Erickson, E. *et al.* (2022) Sourcing thermotolerant poly(ethylene terephthalate) hydrolase scaffolds from natural diversity. *Nat. Commun.* 13, 7850
77. Graham, R. *et al.* (2026) Enhanced enzymatic hydrolysis of pretreated polyester textile at high solids loading through fusion with a carbohydrate binding module. *Bioresour. Technol.* 446, 134174

STAR★METHODS

Key resources table

REAGENT or RESOURCE	SOURCE	IDENTIFIER
Bacterial and virus strains		
Pseudomonas umsongensis GS	This work	
Pseudomonas umsongensis HM2	This work	
Rhodococcus sp. HM1	This work	
Acinetobacter schindleri LK1	This work	
Pseudomonas azerbaijanoccidens SH	This work	
Ralstonia insidiosa TS	This work	
Pseudomonas putida KT2440	Lab collection	NCBI Taxonomy ID: 160488
Piscinobacter sakaiensis	Lab collection	NCBI Taxonomy ID: 1547922
Escherichia coli TOP10	Thermo Fisher Scientific	
Escherichia coli BL21(DE3)	New England Biolabs	
Escherichia coli MG1655	Lab collection	NCBI Taxonomy ID: 511145
Chemicals, peptides, and recombinant proteins		
Amorphous PET	Goodfellow	ES301450
1,1,1,3,3,3-hexafluoroisopropanol (HFIP)	Sigma-Aldrich	105228
p-nitrophenylbutyrate	Sigma-Aldrich	N9876
Bis(2-hydroxyethyl) terephthalate (BHET)	Sigma-Aldrich	465151
Polycaprolactone	Sigma-Aldrich	440744
Critical commercial assays		
Quant-iT dsDNA HS kit	Invitrogen	Q330120
Quick Start Bradford Protein Assay Kit 1	Bio-Rad	#5000201EDU
QIAprep Spin Miniprep Kit – Plasmid Purification	Qiagen	27104
Nextera XT Library Prep Kit	Illumina	FC-131-1024
Deposited data		
Genome sequence *A. schindleri* LK1	This work	JALPTA000000000
Genome sequence *Rhodococcus* sp. HM1	This work	JALPTB000000000
Genome sequence *P. umsongensis* HM2	This work	JALPTC000000000
Genome sequence *P. azerbaijanoccidens* SH	This work	JALPTD000000000
Genome sequence *P. umsongensis* GS	This work	JALPTE000000000
Genome sequence *R. insidiosa* TS	This work	JALPTF000000000
Proteome *P. putida*	Uniprot	UP000000556_160488
Proteome *P. umsonsensis*	Uniprot	UP000215455_198618
Recombinant DNA		
Plasmids	This work	Table S4 (in the Supplemental information online)
Oligonucleotides	Eurofins MWG Operon, Sigma-Aldrich	Table S5 (in the Supplemental information online)
Software and algorithms		
GraphPad Prism 11	GraphPad	https://www.graphpad.com/
ApE	Wayne Davis	https://jorgensen.biology.utah.edu/wayned/ape/
Trimmomatic 0.30	Github	Bolger *et al.*[70]

(continued)

REAGENT or RESOURCE	SOURCE	IDENTIFIER
SPAdes version 3.7	Github	Bankevich *et al.*[71]
Prokka 1.11	Github	Seemann T.[72]
Profinder	Agilent	B.08.00 suite
ProteoScape	Bruker	
Blast	NCBI	https://blast.ncbi.nlm.nih.gov/Blast.cgi
OpenLab	Agilent	
Other		
HT sequencer	Illumina	HiSeq 2500
Freezer/Mill	SPEX SamplePrep	6875
Differential Scanning Calorimeter	Netzsch	DSC214 Polyma
Microplate reader	BMG	Clariostar
UHPLC	Agilent	1290 Infinity II
Mass spectrometer	Agilent	6545 LC/Q QTOF
Mass spectrometer	Evosep	Evosep One
HPLC	Agilent	1260 Infinity II LC
Waste water samples	Road gully in South Kensington (London; UK)	

EXPERIMENTAL MODEL AND STUDY PARTICIPANT DETAILS

Strain isolation

Soil samples were collected from a range of locations at the University of Surrey campus, UK. Bacterial isolates were cultured from these samples by incubation in 5 mL of 1X M9 minimal medium (5X M9 salts (Sigma) 200 mL/L, 1 M $MgSO_4$ 200 µL/L, 1 M $CaCl_2$ 100 µL/L, 1,000X trace element solution ($ZnSO_4 \cdot 7H_2O$ 0.1 g/L, $MnCl_2 \cdot 4H_2O$ 0.03 g/L, H_3BO_3 0.3 g/L, $CoCl_2 \cdot 6H_2O$ 0.2 g/L, $CuCl_2 \cdot 2H_2O$ 0.01 g/L, $NiCl_2 \cdot 6H_2O$ 0.02 g/L, $Na_2MoO_4 \cdot 2H_2O$ 0.03 g/L) 1 mL/L, 10,000X vitamin solution (nicotinic acid 0.01 g/mL, thiamine 0.005 g/L, *p*-aminobenzoic acid 0.001 g/mL, biotin 0.1 mg/mL) 100 µL/L) supplemented with 10 mM TA. Cultures were incubated for 24 h at 30°C. 100 µL of grown cultures were transferred to 5 mL of fresh M9 medium with 10 mM TA in three successive passes. Culturable isolates were streaked in M9-agar plates with 10 mM TA to isolate individual colonies. Monocultures were maintained on LB agar at 30°C.

Whole-genome sequencing and analysis

Whole-genome sequencing of environmental isolates was conducted by MicrobesNG, Birmingham, United Kingdom. Briefly, cells were recovered from a LB plate containing pure cultures of each isolate and transferred to a tube containing DNA/RNA Shield (Zymo Research, USA) following MicrobesNG strain submission procedures. 5 to 40 µL of the suspension were lysed with 120 µL of TE buffer containing lysozyme (final concentration 0.1 mg/mL) and RNase A (ITW Reagents, Barcelona, Spain; final concentration 0.1 mg/mL), incubated for 25 min at 37°C. Proteinase K (VWR Chemicals, Ohio, USA) (final concentration 0.1mg/mL) and SDS (Sigma-Aldrich, Missouri, USA) (final concentration 0.5% v/v) were added and incubated for 5 min at 65°C. Genomic DNA was purified using an equal volume of SPRI beads and resuspended in EB buffer (Qiagen, Germany). DNA was quantified with the Quant-iT dsDNA HS kit (ThermoFisher Scientific, United Kingdom) assay in an Eppendorf AF2200 plate reader (Eppendorf UK Ltd, United Kingdom).

Genomic DNA libraries were prepared using the Nextera XT Library Prep Kit (Illumina, San Diego, USA) following the manufacturer's protocol with the following modifications: input DNA was increased 2-fold, and PCR elongation time was increased to 45 s. DNA quantification and library preparation were carried out on a Hamilton Microlab STAR automated liquid handling system (Hamilton Bonaduz AG, Switzerland). Pooled libraries were quantified using the Kapa Biosystems Library Quantification Kit for Illumina. Libraries were sequenced using Illumina sequencers (HiSeq/NovaSeq) using a 250 bp paired end protocol. Reads were adapter trimmed using Trimmomatic 0.30 with a sliding window quality cutoff of Q15 [70]. De novo assembly was performed on samples using SPAdes version 3.7 [71], and contigs were annotated using Prokka 1.11 [72].16S rRNA regions were used for sequence identification using the NCBI BLAST blastn search tool.

Assembled genomes provided by MicrobesNG were annotated using Rapid Annotation using Subsystem Technology (RAST) to predict CDS regions and protein functions. The NCBI BLASTp tool was used to align query sequences of TA metabolism genes to predicted protein sequences found in the environmental isolates. The genomes were uploaded to the NCBI's GenBank with the following accession numbers: JALPTA000000000 (*A. schindleri* LK1), JALPTB000000000 (*Rhodococcus* sp. HM1), JALPTC000000000 (*P. umsongensis* HM2), JALPTD000000000 (*P. azerbaijanoccidens* SH), JALPTE000000000 (*P. umsongensis* GS), JALPTF000000000 (*R. insidiosa* TS).

Microbial culturing

Environmental isolates were assayed for growth on TA and EG monomers using 1X M9 minimal medium supplemented with 10 mM of each respective monomer (unless stated otherwise). Growth assays were performed at 100 µL volumes in 96-well flat-bottomed microtitre plates using a starting inoculum at OD_{600} ~ 0.01. Plates were incubated at 30°C in a microplate reader (BMG Clariostar) with continuous orbital shaking and OD_{600} readings were taken at 15 min intervals for 72 h.

Routine cell culturing took place in LB medium (Sigma) supplemented with the following antibiotics as required: ampicillin (100 µg/mL), kanamycin (50 µg/mL), chloramphenicol (35 µg/mL), gentamicin (20 µg/mL), streptomycin (100 µg/mL) and tetracycline (10 µg/mL) and 1.5% agar for solid culturing. Supernatants containing secreted enzymes were generated by growing cells for 2 days in LB broth at room temperature. Supernatants were recovered after removing the cells by centrifuging the cultures for 10 min at 12,000 rpm and filtering the supernatants using 0.2 µm cellulose filters (brand Acrodisc). For experiments analysing the growth of *P. umsongensis* GS using PET as a substrate, 10 mg of solvent-pretreated PET was submerged in 20 mL of M9 medium supplemented with the appropriate concentration of LB. For strains expressing PET hydrolases, cultures were additionally supplemented with 50 µg/mL kanamycin and 0.5 mM sodium benzoate for induction. Prior to use, all PET materials were washed with 70% (v/v) ethanol, rinsed thoroughly with sterile water, and air-dried under sterile conditions. Cultures were incubated at 30°C with orbital shaking at 170 rpm, and growth was monitored by measuring OD_{600}.

For initial assessment of nutrient supplementation, M9 medium containing 10%, 50%, or 100% LB was tested, with OD600 measured after 7 days of incubation in the presence and absence of solvent-pretreated PET. Growth kinetics of *P. umsongensis* GS was further assessed over a 4-week period in M9 supplemented with 10% LB, with and without solvent-pretreated PET, and samples were collected every 7 days for OD600 measurements. Viable cell counts were determined by sampling cultures, performing serial dilutions, and plating 10 µL onto LB agar supplemented with kanamycin. Plates were incubated at room temperature until spots had dried and then at 30°C for 48 h before colonies were counted to quantify colony-forming units (CFU). For the 4-week growth analysis, *I. sakaiensis* was included as a positive control. Inoculum cultures were grown in NBRC 802 medium (1.0% polypeptone, 0.2% yeast extract, 0.1% $MgSO_4$) or on NBRC 802 plates solidified with 1.5% agarose. Cultures were incubated under the same conditions as described for *P. umsongensis* GS, and growth was assessed by OD_{600} and CFU measurements as described above.

METHOD DETAILS

PET pretreatment

Cryomilled PET was generated using a SPEX 6875 Freezer/Mill. Amorphous PET films (Goodfellow, ES301450, UK) were cut into 1 cm^2 pieces and subjected to two milling cycles of 2 minutes each at 12 RPS, with 4 minutes of pre-cooling prior to milling. The resulting cryomilled material was passed through a 150-mesh stainless steel sieve (corresponding to a nominal particle size cut-off of ~100 µm) to obtain PET microplastics smaller than 100 µm.

An amorphous, microporous form of PET was produced through solvent pretreatment. Briefly, 1 g of biaxially oriented Goodfellow PET film was dissolved in 10 mL of 1,1,1,3,3,3-hexafluoroisopropanol (HFIP) and added dropwise to 500 mL of isopropanol pre-cooled to –20°C under continuous stirring. The resulting precipitate was collected by filtration, washed thoroughly with isopropanol, and dried at room temperature for 24 h prior to use.

Polymer differential scanning calorimetry

Thermal properties of PET samples, including the glass transition temperature (T_g), melting temperature, and degree of crystallinity, were determined by differential scanning calorimetry using a DSC 214 Polyma instrument (Netzsch). Samples (5-10 mg) were sealed in aluminium pans and subjected to heating from 25°C to 300°C at a constant rate of 10°C min^{-1} under a nitrogen atmosphere.

Thermograms were analysed by integrating the relevant endothermic and exothermic transitions, and the resulting enthalpy values (J g^{-1}) were used to calculate polymer crystallinity according to the equation: % crystallinity = (H - Hc)/ H^{0}, where ΔH is the enthalpy of melting of the sample, ΔH*c* is the enthalpy of crystallisation, and ΔH^{0} is the enthalpy of melting of a theoretically 100% crystalline PET sample, taken as 140.1 J g^{-1}. All data processing and analysis were performed using Proteus Analysis software.

Plasmid assembly and strain engineering

Genetic constructs for plasmid-based expression of genes of interest were assembled using the broad-host pSEVA238 backbone [73] (Table S2, in the Supplemental information online). The plasmid was modified to include a short sequence in the N-terminus of the cloned esterases encoding the peptide leader of the UxpB protein of *P. putida* KT2440. This was achieved by PCR amplifying the secretion leader at the 5' end of uxpB with primers uxpB-Fwd and uxpB-Rev (Table S3, in the Supplemental information online) and conducting Gibson assembly (New England Biolabs, USA) of the resulting fragment into pSEVA238 previously digested with SacI and KpnI. The genes encoding the hydrolases *Tf*Cut2, *TCur*0390, IsPETase, DuraPETase, MHETase and MHETase-PETase (Table S4) were PCR amplified with the appropriate primers (Table S3) using plasmids for intracellular expression as templates (Table S2). The inactive variant *Tf*Cut2mut of *Tf*Cut2 containing the substitution S187A in the active site was generated by overlapping PCR of the whole plasmid containing the wild type gene using the primers described in Table S3. All esterase coding fragments, including LCC (obtained by digestion of pET20-LCC) and DuraPETase (obtained by DNA synthesis) were cloned in the vector using restriction enzymes BamHI and HindIII followed by ligation with T4 DNA ligase. All Gibson and ligation mixtures were transformed into *E. coli* TOP10 competent cells and selected on LB agar supplemented with kanamycin.

Plasmids were delivered to *E. coli* MG1655 by electroporation in preparation for enzymatic assays. Plasmids were also transferred from *E. coli* to the environmental isolates by triparental mating using *E. coli* DH5α carrying the appropriate plasmids as donors and *E. coli* HB101 pRK600 as a helper [74]. Transconjugants were selected in M9 medium containing 5 mM of TA as the only carbon source (selective for the recipient strains) and kanamycin.

Esterase enzymatic assays and TA determination

Degradation of PET nanoparticles was conducted in LB-agar plates containing PET nanoparticles prepared as described previously (Pütz, A.PhD thesis, Heinrich Heine University Düsseldorf, 2006). In short, 0.1 g of PET was dissolved in 10 ml HFIP and precipitated by dropping the solution into 100 mL of ice-cold water under stirring and subsequent concentration under vacuum. 100 mg of the nanoparticles were added to 500 mL of molten agar media prior to pouring into Petri dishes. Plates were inoculated with single colonies of esterase producing strains and incubated for 2 days at 30°C followed by 1-day long incubation at 50°C (for assays with thermophilic cutinases). PCL plates were prepared by dissolving 250 mg of PCL in 30 mL of acetone and incubating at 50°C until complete solubilisation. The suspension was mixed slowly with 500 mL of molten LB agar and sonicated in a water bath for 15 minutes before adding any required antibiotics or inducers prior to pouring in petri dishes. Plates were left to dry in a sterile cabinet to allow acetone to evaporate.

Hydrolysis of *p*NPB was conducted using culture supernatants of *E. coli* MG1655 cells [75] grown on LB. Strains containing plasmids for the production and secretion of esterases were cultured to saturation for 14 h. 1 mL of culture supernatants was collected and cells were removed by centrifugation 10 min at 13,000 rpm followed by filtering with a 0.2 µL syringe filter (Fisher Scientific). Protein concentration in the supernatants was determined using colorimetric Protein Assay (Bio-Rad). All assays were conducted with a volume of freshly prepared supernatant containing 10 ng of total protein (typically in the range of 10 µL) added to a mixture of 80 µL of phosphate buffer 100 mM pH 8.0 and 10 µL of 5 mM *p*NPB in 96-well plates (total volume 100 µL per reaction). Reactions were incubated at 30 or 42°C and monitored measuring the increase in absorbance at 405 nm in a microplate reader (Infinite m200 Pro; Tecan). The absorbance of a control containing *p*NPB in the reaction buffer, but lacking culture supernatant was monitored in the same conditions to determine the spontaneous hydrolysis of the substrate. These values were considered background and subtracted from the absorbance of the test samples. The reactions were monitored over time and initial linear absorbance values were fitted by linear regression (GraphPad Prism) to obtain the initial reaction velocities.

For enzymatic PET degradation we used either 1 cm^2 of amorphous films with a thickness of 0.25 mm (Goodfellow, UK), 0.1 g of the same PET cryomilled in advance, 0.1 g of cryomilled PET sieved at <100 µm or 10 mg of solvent-pretreated PET. Plastics were submerged in 1 mL LB culture supernatants containing 5 µg/mL of total protein previously determined in a Bradford Assay (Bio-Rad). Incubations took place

at 30°C for 3 weeks. TA released and accumulated in the supernatants was determined spectrophotometrically at 240 nm on a routine basis.

TA was also determined by ultra-high performance liquid chromatography followed by mass spectrometry (HPLC-MS). The data were acquired with an Agilent 1290 Infinity II UHPLC coupled to a 6545 LC/Q QTOF system. Chromatographic separation was performed with an Agilent InfinityLab Poroshell 120 HILIC-Z (2.1 × 100 mm, 2.7 µm (p/n 675775-924)) column. A concentrated 10x solution consisting of 100 mM ammonium acetate (pH 9.0) in water was prepared to produce mobile phases A and B. Mobile phase A consisted of 10 mM ammonium acetate in water (pH 9) with a 5-µM Agilent InfinityLab Deactivator Additive (p/n 5191-4506), and mobile phase B consisted of 1.0 mM ammonium acetate (pH 9) in 10:90 (v:v) water/acetonitrile with a 5-µM Agilent InfinityLab Deactivator Additive (p/n 5191-4506). The following gradient was applied at a flow rate of 0.5 ml/min: 0 minutes, 100% B; 0-11.5 minutes, 70% B; 11.5-15 minutes, 100% B; 12-15 minutes, 100% B; and 5-minutes of re-equilibration at 100% B. Dynamic mass axis calibration was achieved by continuous infusion after the chromatography of a reference mass solution using an isocratic pump connected to an ESI ionization source operated in negative-ion mode. The following parameters were used: sheath gas temperature, 300°C; nebulizer pressure, 40 psi; sheath gas flow, 12 l min-1; capillary voltage, 3000 V; nozzle voltage, 0 V; and fragmentor voltage, 115 V. The data were collected in centroid 4 GHz (extended dynamic range) mode. Data was analysed with the Agilent's Profinder B.08.00 suite (mass 166.0266).

PHL7 expression optimisation

Overnight cultures of recombinant *P. umsongensis* GS PHL7-expressing cells were grown in LB medium supplemented with 50 µg/mL kanamycin at 30°C with shaking. The following day, cultures reached an OD600 of ~5. For induction experiments, 100 µL of the overnight culture was used to inoculate 900 µL of fresh LB medium supplemented with sodium benzoate to achieve final concentrations of 0.00, 0.05, 0.10, 0.25, 0.50, 0.75, 1.00, and 2.00 mM in a total culture volume of 1 mL. Cultures were incubated in 96-well plates at 30°C with shaking at 180 rpm for 2 days. After incubation, plates were centrifuged at 13,000 rpm for 20 min to pellet the cells. 500 µL of supernatant was carefully removed and filtered through 0.22 µm spin columns by centrifugation at 13,000 rpm for 10 min. All assays were performed with freshly prepared solutions.

Enzyme activity was measured using a *p*NPB assay. For each reaction, 10 µL of filtered supernatant was added to 80 µL of 100 mM phosphate buffer (pH 8.0) and 10 µL of 5 mM *p*NPB (dissolved in anhydrous DMSO and added last) to give a total reaction volume of 100 µL in a 96-well plate. Reactions were incubated at 30°C, and absorbance at 405 nm was monitored using a Tecan plate reader as shown in the previous section. Controls included buffer plus *p*NPB with no supernatant to account for any non-enzymatic hydrolysis of the substrate. Absorbance from control wells was subtracted from sample wells before calculating initial rates. The initial rate for each replicate was calculated from the slope of absorbance versus time using linear regression and are reported as ΔA_{405} min^{-1}. Graphs show mean initial rates ± SD. Statistical significance between inducer concentrations was determined by one-way ANOVA followed by Tukey's multiple comparisons test, with $p < 0.05$ considered significant.

PHL7 proteomic determination

WT and PHL7-expressing *P. umsongensis* GS strains were streaked onto LB agar plates, with kanamycin (50 µg mL^{-1}) added for maintenance of the expression plasmid where appropriate, and incubated overnight at 30°C. Single colonies were used to inoculate 50 mL M9 minimal medium containing 0.4% (w/v) glucose and antibiotic (PHL7-expressing strain) and incubated overnight at 30°C with shaking at 180 rpm. Overnight cultures were used to inoculate fresh M9 minimal medium containing 0.4% (w/v) glucose and 0.5 mM sodium benzoate in 100 mL Erlenmeyer flasks to a final working volume of 30 mL. Media were supplemented with kanamycin (50 µg mL^{-1}) for the PHL7-expressing strain only. Cultures were incubated at 30°C with shaking at 180 rpm for 48 h to allow enzyme secretion, with samples collected at 0, 24 and 48 h. Cells were removed by centrifugation (4,000 x g, 10 min), and culture supernatants were filtered through 0.22 µm syringe filters to remove residual cells. Aliquots (200 µL) of 48 h supernatants from both WT and PHL7-expressing strains were subjected to reduction and alkylation by addition of 0.5 volumes each of TCEP and chloroacetamide, followed by incubation at room temperature for 10 min. Proteins were precipitated by the addition of acetonitrile and washed with ethanol prior to digestion with sequencing-grade trypsin (25 µL of 14 ng μL^{-1} trypsin in 25 mM ammonium bicarbonate). Samples were incubated overnight at 37°C with shaking at 600 rpm. Digests were dried using a SpeedVac concentrator for approximately 30 min, reconstituted in 20 µL of 0.1% formic acid, and adjusted to a peptide concentration of 10 ng μL^{-1}. Peptides were submitted for LC-MS/MS analysis to Imperial College 4D-Proteomics Facility.

Samples were analysed using an Evosep One (Evosep) coupled to a timsTOF HT (Bruker) equipped with an Evosep Performance EV1109 analytical column (8 cm x 150 µm, 1.5 µm). Peptides (200 ng per sample) were loaded onto Evotips according to manufacturer's instruction and separated using the Evosep 60-samples-per-day (60SPD) workflow. Analytical solvents were A: 0.1% formic acid and B: acetonitrile with 0.1% formic acid). The column temperature was maintained at 40°C. Data were acquired in dia-PASEF mode with the following parameters: m/z range from 100 - 1700, ion mobility range $1/K_0$ = 1.30 - 0.85 Vs cm^{-2} using equal ion accumulation and ramp times of 100 ms in the dual TIMS analyser. Each cycle consisted of eight PASEF ramps covering 21 mass steps (25 Da windows) with 2/3 non-overlapping ion mobility windows spanning the 475 - 1000 m/z range and 0.85 - 1.26 Vs cm^{-2} ion mobility range. Collision energy was decreased as a function of increasing ion mobility from 59 eV at $1/K_0$ = 1.6 Vs cm^{-2} to 20 eV at $1/K_0$ = 0.6 Vs cm^{-2}.

LC-MS/MS data were processed using the real-time processing platform ProteoScape (Bruker) with the workflow 'dia-PASEF-RT Spectronaut19'. Reference proteomes for *P. putida* (UP000000556_160488) and *P. umsongensis* (UP000215455_198618) were downloaded from Uniprot and combined with the PHL7 sequence into a single FASTA file for database searching. Search parameters were Trypsin/P with Vs cm^{-2} to two missed cleavages; carbamidomethylation (C) as a fixed modification, oxidation, and N-terminal acetylation as variable modifications (maximum five variable modifications). Protein identifications were accepted at a Q-value (FDR) threshold of 0.01. All other parameters were left at default settings.

PHL7 polyacrylamide gel electrophoresis (PAGE) and activity assays

For concentrated samples, clarified 48 h supernatants from the previous section were reduced to ~2 mL using 10 kDa molecular weight cut-off centrifugal concentrators. Protein concentration of the PHL7-expressing supernatant was estimated by absorbance at 280 nm using a BioDrop spectrophotometer and measured at approximately 0.5 mg mL^{-1}. WT supernatants were concentrated to the same final volume; however, protein levels remained low due to limited native protein secretion.

Unconcentrated and concentrated supernatants were analysed by SDS-PAGE using precast polyacrylamide gels (Bio-Rad, 10-well format) run at constant voltage for approximately 50 min. Precision Plus Dual Color Standard (5 µL; Bio-Rad) was used as a molecular weight marker. The leaf-branch compost cutinase variant LCC^{ICCG} (27.6 kDa) was included as a protein control due to its similar molecular weight to PHL7 (27.8 kDa), as purified PHL7 was not available. Gels were stained overnight using SimplyBlue SafeStain (Invitrogen) and rinsed with ultrapure water. The protein band observed in the 48-h sample was excised using a sterile scalpel, cut into 1-2 mm fragments, and prepared for in-gel digestion. Gel pieces were transferred to low-bind tubes and destained using 25 mM ammonium bicarbonate in 50% (v/v) acetonitrile at 37°C with gentle agitation until clear. Samples were dehydrated with acetonitrile and briefly air-dried prior to rehydration in trypsin solution (1 µg trypsin in 100 µL water). Digestion buffer (25 mM ammonium bicarbonate) was added, and samples were incubated at 30°C overnight with agitation. Extracted peptides were analysed by LC-MS/MS as described above to confirm protein identity as described above.

Hydrolytic activity of secreted enzymes was assessed using agar plates containing BHET. Agarose (1 g) was dissolved in 40 mL of 0.1 M phosphate buffer by heating, and finely powdered BHET (0.3 g) was suspended in 10 mL distilled water before being added to cooled agarose solution. The mixture was poured into Petri dishes and allowed to solidify. Wells were created using a sterile borer, and 40 µL of filtered 48 h culture supernatants, concentrated or unconcentrated, from WT or PHL7-expressing strains were added. Plates were incubated at 30°C for 48 h, and hydrolysis was indicated by clear halos surrounding wells, with WT samples serving as negative controls. LCC^{ICCG} was included as a positive control due to its known ability to produce clearance halos on BHET agar plates.

Environmental wastewater PET microplastic degradation

Reaction assays were performed in 14 mL round-bottom Falcon culture tubes. Each reaction contained 20 mg cryomilled PET microplastics and a final working volume of 2 mL. Wastewater was collected from the waste trap of a gully drain in South Kensington (London; UK), used without sterilisation, and processed as collected. Cryomilled PET was sieved through a 150-mesh screen to obtain particles <100 µm. For each reaction, 1.9 mL wastewater was added to the tube together with 20 mg PET. Wastewater was supplemented with sodium benzoate (0.5 mM final concentration) to induce PHL7 expression.

WT *P. umsongensis* GS and the corresponding PHL7-expressing strain were prepared by streaking onto LB agar (WT) or LB agar supplemented with kanamycin (50 µg/mL; PHL7 strain) and incubating overnight. For control experiments, *I. sakaiensis* cultures

grown in YSV medium consisting of 0.01% yeast extract, 0.02% sodium bicarbonate, 0.1% ammonium sulphate, 0.01% calcium carbonate, 0.1% vitamin mixture (containing 0.25% thiamine-HCl, 0.005% biotin, and 0.05% vitamin B12), and 1% trace elements prepared in 10 mM phosphate buffer (pH 7.0) and wastewater were prepared in parallel. Single colonies were used to inoculate 50 mL M9 minimal medium containing 0.4% (w/v) glucose, followed by incubation at 30°C and 180 rpm overnight. Cultures were adjusted to OD_{600} = 1.0 prior to inoculation. Each reaction was inoculated with 100 µL of adjusted culture, giving a final volume of 2 mL and a starting OD_{600} of approximately 0.5 (5% v/v inoculum). Tubes were incubated at 30°C with shaking at 180 rpm for up to 720 h.

Sampling was performed by removing 200 µL of well-mixed reaction slurry immediately after inoculation (t = 0), followed by sampling every 24 h up to 96 h (24, 48, 72, and 96 h), with additional samples collected at 168 h or 192 h and 720 h. After each sampling event, the reaction volume was restored by adding 200 µL of replacement medium consisting of wastewater prepared to match the original condition (including LB, kanamycin, and/or sodium benzoate where applicable, at the same final concentrations: 10% LB, 50 µg/mL kanamycin, 0.5 mM sodium benzoate). This ensured a constant working volume of 2 mL and constant nominal supplement concentrations throughout the experiment.

Samples were heat-treated at 95°C to terminate biological activity and centrifuged at 14,000 rpm for 10 min to remove particulates. Samples were then clarified using 0.22 µm Costar Spin-X centrifuge tube filters and stored at 4°C prior to HPLC analysis of soluble PET-derived degradation products. Quantification of mono-aromatic PET hydrolysis products, including TA, MHET and BHET, was performed by HPLC as previously described [76,77] and summarised here: Samples were diluted (typically 1/10) to fall within the linear range of detection. HPLC analysis was performed using an Agilent 1260 Infinity II LC system equipped with a diode array detector monitoring at 240 nm. Analytes were separated on a guard-equipped C18 Kinetex column (00B-4605-AN) pre-equilibrated with mobile phase at a flow rate of 1.1 mL min^{-1}. Mobile phase solvents consisted of 0.1% FA in water (solvent A) and acetonitrile (solvent B), with the following gradient: isocratic elution at 13% B for 0.87 min, column washing at 95% B for 1.12 min, followed by re-equilibration at 13% B for 1.61 min. To minimise carryover between sample sets, 95% acetonitrile was periodically injected to clean the column. Chromatographic peaks were integrated using Agilent OpenLab software, and compound concentrations were determined using calibration curves generated from authentic standards.

For endpoint biomass measurements, 200 µL of culture supernatant collected at 720 h was analysed by optical density at OD_{600} using a CLARIOstar plate reader (BMG Labtech) in a 96-well plate.

Violacein determination

Violacein present in culture supernatants was determined as described follows [36]. Briefly, cells were recovered by centrifugation (13,000 rpm, 10 min) of 1 mL of culture. Violacein was extracted from the cell pellets with 1 mL absolute ethanol incubating at 95°C for 10 min followed by removal of pellets by centrifugation (13,000 rpm, 10 min). Violacein in supernatants was determined reading absorbance at 570 nm in a BMG Clariostar microplate reader.

QUANTIFICATION AND STATISTICAL ANALYSIS

All results show the mean of at least three independent biological replicates with three technical each unless stated otherwise. Evaluation of significant differences was assessed by conducting a one-way ANOVA with a post-hoc Dunnett test or a two-tailed t-test when required as shown in figure captions. Pairwise comparisons were always conducted against the negative control for the experiment. Absence of asterisks in the plots represents no significant differences, while p-values are represented as: **** $p<0.0001$; *** $p<0.001$; ** $p<0.01$; * $p<0.1$.